

Accepted Manuscript

A close insight into the nature of inter- and intermolecular interactions in new Cu(II) Schiff base complexes derived from halogenated salicylaldehydes and allylamine: Theoretical and crystallographic studies

Mahnaz Aryaeifar, Hadi Amiri Rudbari, Giuseppe Bruno

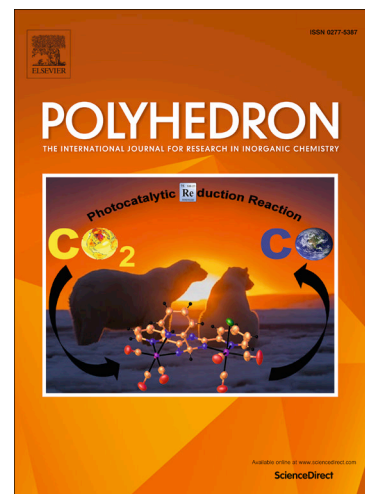
PII: S0277-5387(18)30489-3
DOI: <https://doi.org/10.1016/j.poly.2018.08.023>
Reference: POLY 13346

To appear in: *Polyhedron*

Received Date: 10 May 2018
Accepted Date: 10 August 2018

Please cite this article as: M. Aryaeifar, H. Amiri Rudbari, G. Bruno, A close insight into the nature of inter- and intermolecular interactions in new Cu(II) Schiff base complexes derived from halogenated salicylaldehydes and allylamine: Theoretical and crystallographic studies, *Polyhedron* (2018), doi: <https://doi.org/10.1016/j.poly.2018.08.023>

This is a PDF file of an unedited manuscript that has been accepted for publication. As a service to our customers we are providing this early version of the manuscript. The manuscript will undergo copyediting, typesetting, and review of the resulting proof before it is published in its final form. Please note that during the production process errors may be discovered which could affect the content, and all legal disclaimers that apply to the journal pertain.



A close insight into the nature of inter- and intermolecular interactions in new Cu(II) Schiff base complexes derived from halogenated salicylaldehydes and allylamine: theoretical and crystallographic studies

Mahnaz Aryaeifar ^a, Hadi Amiri Rudbari ^{a,*}, Giuseppe Bruno ^{b,*}

^a *Department of Chemistry, University of Isfahan, Isfahan 81746-73441, Iran.*

^b *Department of Chemical Sciences, University of Messina, Via F. Stagno d'Alcontres 31, 98166 Messina, Italy.*

***Corresponding authors:**

E-mail addresses: h.a.rudbari@sci.ui.ac.ir, hamiri1358@gmail.com (H. Amiri Rudbari); gbruno@unime.it (G. Bruno).

Abstract:

Although numerous Schiff base complexes have been synthesized and characterized, reports on Schiff base ligands and complexes derived from amines containing terminal allyl group are rare. In this work, four halogenated Schiff base compounds were synthesized by reaction of halogenated salicylaldehydes (3,5-dichlorosalicylaldehyde, 3,5-dibromosalicylaldehyde, 3,5-diiodosalicylaldehyde and 3-bromo-5-chlorosalicylaldehyde) with allyl amine in water as green solvent at ambient temperature and characterized by elemental analyses, NMR (^1H and ^{13}C), and FT-IR spectroscopy. In continue, their Cu(II) complexes were synthesized and characterized by elemental analyses, FT-IR and single-crystal x-ray diffraction. All complexes show halogen-halogen, π - π , CH- π interactions and also metal-halogen secondary bonds in crystal packing. The coordination geometry around the Cu(II) in all reported compounds is best described as square planar with two axially elongated interactions named metal-halogen secondary bond (Cu...X), all beyond the sum of the corresponding vdW radii (3.421 Å for Cu...Cl in $(\text{Cl}_2\text{L})_2\text{Cu}$, 3.463 Å for Cu...Br in $(\text{Br}_2\text{L})_2\text{Cu}$, 3.486 Å for Cu...I in $(\text{I}_2\text{L})_2\text{Cu}$ and 3.467 Å for Cu...Cl in $(\text{BrClI})_2\text{Cu}$). The crystal structures have also been subjected to Hirshfeld surface analysis which reveals that approximately most of the close contacts correspond to relatively weak interactions. Also, all of the interactions in crystal packing have been analyzed by theoretical calculations.

1. Introduction

Halogen atoms are common substituents in a highly diverse range of molecules and subject to noncovalent interactions in both solution and the solid state. The halogen bond occurs when there is evidence of a net attractive interaction between an electrophilic region associated with a halogen atom in a molecular entity and a nucleophilic region in another, or the same, molecular entity.

The polarizable halogens exhibit electrophilic δ^+ character along the axis of the C–X bond developing “the positive σ -hole” and nucleophilic δ^- character perpendicular to C–X bond, referred to as the “belt” (Fig. 1) [1].

Halogen atoms undergo three kinds of weak non-covalent interactions, specifically halogen bonding, halogen–halogen interactions, and halogen– π interactions (Scheme 1) [2, 3]. Investigation of halogen bonding (a in scheme 1) in biomolecules, halogenated alkanes, halogenated phenols, and host molecule–polymer macromolecules by relying on crystallography data show that halogens have a tendency to form Lewis acid-base pairs with both electron acceptors and electron-donating heteroatoms, yielding bond angles between 140 – 180° and bond lengths of less than the sum of the van der Waals radii [4].

In the halogen–halogen interactions ($X\cdots X$) (b in scheme 1), both halogen bond donor and acceptor are halogen atoms [5]. This requires one of the halogen atoms to develop a positive electrostatic potential, i.e. a positive σ -hole interacting with an electron rich region (a negative belt) of another [6]. The anisotropic electron distribution around the halogen atom bonded to the carbon atom facilitates this electrophile– nucleophile pairing interaction [7]. Halogen...halogen interactions ($C-X_1\dots X_2-C$) are characterized in terms of three parameters, $R_{ij} = X_1\dots X_2$ and two angles $\theta_1 = C-X_1\dots X_2$ and $\theta_2 = X_1\dots X_2-C$ (b in scheme 1). Type I geometries can be

thought to give rise to an electrostatically repulsive arrangement since at the point of interaction on their molecular surfaces the electrostatic potentials are approximately identical. By contrast, type II geometries are consistent with the description of halogen bonds, wherein the two halogens have distinct and different roles: one halogen provides the Lewis basic site (the halogen bond acceptor) situated orthogonal to the C—X bond and this is aligned in a linear arrangement with the Lewis acidic C—X group [8].

The strength of the halogen–halogen interactions formed by the halogen atom depends to the size and charge of the halogen σ -hole. The size and charge of the halogen σ -hole, depends on two key factors, namely the identity of the halogen and the chemical environment in which the halogen is found [9]. Larger halogens tend to form larger (more positive) σ -holes, leading to stronger interactions that are more electrostatic in nature ($I > Br > Cl$) [10]. By contrast, organo-fluorines do not typically display halogen bonding properties due to the small size, extreme electronegativity, and limited polarizability of fluorine atoms.

As mentioned in above, the size of a σ -hole is also strongly affected by the electronegativity of the atoms (or chemical groups) that are located near the C—X bond. The electron withdrawing effects of electronegative atoms tend to lower the overall negative charge on a halogen and, therefore, lead to more positively charged σ -holes. For example, Halogen bonds involving aromatically bound halogens are generally stronger than those of aliphatic halogens because aromatic moieties have electron withdrawing properties that lead to larger σ -holes. Generally, the hybridization of carbons to which halogens are attached affects halogen bonding ability in the order $C(sp)-X > C(sp^2)-X > C(sp^3)-X$ [11].

Halogen- π interactions (c in scheme 1) are non-covalent interactions of aromatic donors with halogenated organic molecules; these are similar to the more common CH- π interactions [12]. These interactions are of importance in the electrophilic halogenation of aromatic systems. Also, in another interaction for halogens, the negatively charged region can interact with the positive charge of a transition metal. These short interactions are classified as “metal-halogen secondary bonds,” which are formally defined as halocarbon complexes having a halogen metal distance considerably below the sum of their van der Waals radii but longer than the metal-halide bond length (Fig. 2)[13-15]. On the basis of nuclear quadrupole resonance (NQR) spectroscopy results, Wulfsberg proposed the criterion that the metal-halogen distance must be shorter than the average metal-halide distance plus 1 Å [16]. As depicted in Fig. 2, this kind of interaction have type II geometry (b in scheme 1). Although this type of metal-halogen interaction is known in coordination chemistry but are relatively rare, and there are few techniques capable of detecting these bonds other than X-ray crystallography and NQR, thereupon little studied. Although numerous Schiff base complexes with different structures have been synthesized and characterized, reports on Schiff base ligands and complexes derived from amines containing terminal allyl group are scanty [17,18]. We have recently reported the synthesis and structural properties some of them [19-22]. In continuation of our research program aiming at the understanding of the role of intra and intermolecular interactions in the allyl metal-containing crystal structures, a series of halogenated Schiff base compounds containing allyl group, in which the halogen atoms are in the phenyl *ortho* and *para* positions, **Cl₂LH**, **Br₂LH**, **I₂LH** and **BrCILH**, have been employed for the synthesis of four new Cu(II) complexes.

2. Experimental Section

2.1. Chemicals and instrumentation

All the chemicals were purchased from Sigma-Aldrich Co. and used without further purification. The FT-IR spectra were recorded on a JASCO, FT/IR-6300 spectrometer (4000–400 cm^{-1}) in KBr pellets. ^1H and ^{13}C NMR spectra were recorded on a Bruker Avance 400 spectrometer using CDCl_3 as solvents for the ligands. The elemental analyses were performed on Leco, CHNS-932 and Perkin-Elmer 7300 DV elemental analyzers.

2.2. Crystallographic refinement details

The X-ray data of $(\text{Cl}_2\text{L})_2\text{Cu}$, $(\text{Br}_2\text{L})_2\text{Cu}$, $(\text{I}_2\text{L})_2\text{Cu}$ and $(\text{BrCIL})_2\text{Cu}$ were collected at room temperature with a Bruker APEX II CCD area detector diffractometer using $\text{Mo K}\alpha$ radiation ($\lambda = 0.71073 \text{ \AA}$). Data collections, cell refinements, data reductions and absorption corrections were performed using multiscan methods with Bruker software [23]. The structures were solved by direct methods using SIR2004 [24]. The non-hydrogen atoms were refined anisotropically by the full matrix least squares method on F^2 using SHELXL [25]. All hydrogen atoms were added at ideal positions and constrained to ride on their parent atoms. Crystallographic data for complexes are listed in Table 1. Selected bond distances and angles are summarized in Table 2.

2.3. Computational study

Theoretical calculations were made in order to understand solid-state interactions that determine molecular packing of our compounds and attempt to quantify the energies of the individual interactions that are predominantly made up by several halogen bond. The Density Functional Theory approach it was also used to test the relatively inexpensive validity of quasi-relativistic

effective core potential. DFT calculations were performed by using the GAUSSIAN 09 program package [26] on i7 processor personal computer. The effect of electron correlation on the molecular geometry was taken into account by using Becke's three-parameter hybrid, and the gradient corrected Lee-Yang-Parr correlational functional (B3LYP) [27] employing the quasi-relativistic effective core potential (RECP) SDD and valence basis sets recommended by Stuttgart group [28]. B3LYP and several other functionals such as HSEH1PBE [29], PBEPBE [30], HCTH [31] were used in conjunction with the standard basis sets (SDD) in order to test their ability to reproduce the interactions energy. Among those, the functional HSEH1PBE, in conjunction with SDD basis sets and the AUTO fitting set it seems to be the best in simulating the regular proceeding of the potential energy curve of the interactions. Energy interaction calculations, as single point energy (SPE), for dimeric couples was computed, starting from the crystal structures geometry of all samples as coming from the x-ray determination, varying the appropriate distance from 2 Å to ∞ . The energy of dimers at infinite distance it was placed equal two time the monomer's energy; this energy was taken as zero. The counterpoise correction [32] is employed to reduce basis set superposition error (BSSE).

2.4. Hirshfeld surface analysis

Hirshfeld surfaces (HSs) and 2D fingerprint plots (FPs) were generated using Crystal Explorer 3.1 [33] based on results of single crystal X-ray diffraction studies. The function d_{norm} is a ratio encompassing the distances of any surface point to the nearest interior (d_i) and exterior (d_e) atom and the van der Waals radii of the atoms [34,35]. The negative value of d_{norm} indicates the sum of d_i and d_e is shorter than the sum of the relevant van der Waals radii, which is considered to be a closest contact and is visualized as red color in the HSs. The white color denotes intermolecular

distances close to van der Waals contacts with d_{norm} equal to zero whereas contacts longer than the sum of van der Waals radii with positive d_{norm} values are colored with blue. A plot of d_i versus d_e is a 2D fingerprint plot which recognizes the existence of different types of intermolecular interactions.

2.5. Synthesis of the Schiff-base ligands

All Schiff base ligands, **Cl₂LH**: allylamine and 3,5-dichlorosalicylaldehyde; **Br₂LH**: allylamine and 3,5-dibromosalicylaldehyde; **I₂LH**: allylamine and 3,5-diiodosalicylaldehyde; **BrClLH**: allylamine and 3-bromo-5-chlorosalicylaldehyde, were synthesized using identical reaction conditions. Therefore, only the synthesis of **Cl₂LH** will be described in detail. The addition of 10 mmol of 3,5-dichlorosalicylaldehyde to a distilled water solution (20 mL) of allylamine (12 mmol) at room temperature yielded a yellow precipitate almost immediately. The reaction mixture was stirred overnight, then the yellow precipitate was collected by filtration, washed with 50 mL of distilled water, and dried in air.

Cl₂LH: Yield 95%, Anal. calc. for C₁₀H₉Cl₂NO: C: 52.20, H: 3.94, N: 6.09. Found: C: 52.23, H: 3.95, N: 6.07. FT-IR (KBr, cm⁻¹): 1625 (vs, $\nu_{\text{C=N}}$). ¹H NMR (CDCl₃, 400 MHz, 298 K) δ /ppm: 14.51 (s, 1H, OH); 8.28 (s, 1H, N=CH); 7.42 (d, 1H, ClC-CH-CC); 7.17 (s, 1H, ClC-CH-CCl); 6.01 (m, 1H, CH=CH₂); 5.28 (d of q, 1H, CH=CHH); 5.25 (d of q, 1H, CH=CHH), 4.29 (d of q, CH₂CH=CH₂). ¹³CNMR (CDCl₃, 400 MHz, 298 K) δ /ppm: 163.96, 157.43, 133.48, 132.37, 129.00, 123.15, 122.28, 119.38, 117.63, 60.12.

Br₂LH: Yield 92%, Anal. calc. for C₁₀H₉Br₂NO: C: 37.65, H: 2.84, N: 4.39. Found: C: 37.64, H: 2.86, N: 4.39. FT-IR (KBr, cm⁻¹): 1629 (vs, ν_{C=N}). ¹H NMR (CDCl₃, 400 MHz, 298 K) δ/ppm: 14.69 (s, 1H, OH); 8.24 (s, 1H, N=CH); 7.71 (d, 1H, ClC-CH-CC); 7.34 (s, 1H, ClC-CH-CCl); 5.99 (m, 1H, CH=CH₂); 5.27 (d of q, 1H, CH=CHH); 5.25 (d of q, 1H, CH=CHH), 4.28 (d of q, CH₂CH=CH₂). ¹³CNMR (CDCl₃, 400 MHz, 298 K) δ/ppm: 163.80, 159.07, 137.83, 133.37, 132.76, 119.63, 117.76, 112.88, 108.97, 59.82.

I₂LH: Yield 92%, Anal. calc. for C₁₀H₉I₂NO: C: 29.08, H: 2.20, N: 3.39. Found: C: 29.11, H: 2.23, N: 3.40. FT-IR (KBr, cm⁻¹): 1623 (vs, ν_{C=N}). ¹H NMR (CDCl₃, 400 MHz, 298 K) δ/ppm: 14.90 (s, 1H, OH); 8.14 (s, 1H, N=CH); 8.06 (d, 1H, ClC-CH-CC); 7.51 (s, 1H, ClC-CH-CCl); 5.98 (m, 1H, CH=CH₂); 5.28 (d of q, 1H, CH=CHH); 5.25 (d of q, 1H, CH=CHH), 4.27 (d of q, CH₂CH=CH₂). ¹³CNMR (CDCl₃, 400 MHz, 298 K) δ/ppm: 163.49, 162.38, 148.88, 139.90, 133.26, 119.36, 117.93, 89.05, 78.24, 59.40.

BrClLH: Yield 90%, Anal. calc. for C₁₀H₉BrClNO: C: 43.75, H: 3.30, N: 5.10. Found: C: 43.74, H: 3.31, N: 5.08. FT-IR (KBr, cm⁻¹): 1627 (vs, ν_{C=N}). ¹H NMR (CDCl₃, 400 MHz, 298 K) δ/ppm: 14.64 (s, 1H, OH); 8.25 (d, 1H, N=CH); 7.59 (d, 1H, ClC-CH-CC); 7.22 (s, 1H, ClC-CH-CCl); 6.01 (m, 1H, CH=CH₂); 5.30 (d of t, 1H, CH=CHH); 5.25 (d of t, 1H, CH=CHH), 4.29 (d of t, CH₂CH=CH₂). ¹³CNMR (CDCl₃, 400 MHz, 298 K) δ/ppm: 163.85, 158.40, 135.26, 133.44, 129.74, 122.67, 119.05, 117.69, 112.38, 60.00.

2.6. Preparation of the complexes

Similar to ligands, the four complexes were synthesized using identical reaction conditions, therefore only the synthesis of $(\text{Cl}_2\text{L})_2\text{Cu}$ will be described in detail. A solution of triethylamine (3 mmol) in MeOH (5 mL) was added to the MeOH solution (20 mL) of ligand Cl_2LH (2 mmol), the solution turned dark yellow and was stirred for 10 min, then addition of 1 mmol of $\text{CuCl}_2 \cdot 2\text{H}_2\text{O}$ to this solution yielded a green precipitate almost immediately. The resulting was refluxed for 3 h to preparation of the $(\text{Cl}_2\text{L})_2\text{Cu}$ complexes. Then the green precipitate was collected by filtration, washed with methanol, and dried in air. For all four complexes the green crystals were obtained in tetrahydrofuran by recrystallization.

$(\text{Cl}_2\text{L})_2\text{Cu}$: Yield 89%, Anal. calc. for $\text{C}_{20}\text{H}_{16}\text{Cl}_4\text{CuN}_2\text{O}_2$: C: 46.04, H: 3.09, N: 5.37. Found: C: 46.03, H: 3.10, N: 5.37., FT-IR (KBr, cm^{-1}): 1619 (vs, $\nu_{\text{C}=\text{N}}$).

$(\text{Br}_2\text{L})_2\text{Cu}$: Yield 87%, Anal. calc. for $\text{C}_{20}\text{H}_{16}\text{Br}_4\text{CuN}_2\text{O}_2$: C: 34.34, H: 2.31, N: 4.00. Found: C: 34.35, H: 2.33, N: 3.99., FT-IR (KBr, cm^{-1}): 1618 (vs, $\nu_{\text{C}=\text{N}}$).

$(\text{I}_2\text{L})_2\text{Cu}$: Yield 93%, Anal. calc. for $\text{C}_{20}\text{H}_{16}\text{CuI}_4\text{N}_2\text{O}_2$: C: 27.07, H: 1.82, N: 3.16. Found: C: 27.07, H: 1.83, N: 3.16., FT-IR (KBr, cm^{-1}): 1616 (vs, $\nu_{\text{C}=\text{N}}$).

$(\text{BrClL})_2\text{Cu}$: Yield 91%, Anal. calc. for $\text{C}_{20}\text{H}_{16}\text{Br}_2\text{Cl}_2\text{CuN}_2\text{O}_2$: C: 39.34, H: 2.64, N: 4.59. Found: C: 39.33, H: 2.65, N: 4.61., FT-IR (KBr, cm^{-1}): 1619 (vs, $\nu_{\text{C}=\text{N}}$).

3. Result and Discussion

3.1. IR and NMR spectra

Synthesis of Schiff base ligands and their Cu(II) complexes are shown in Schemes 2 and 3. All of complexes were obtained in good yield (more than 90%). The elemental analyses of the complexes were consistent with their proposed compositions. Stability of all ligands and complexes in the most common polar and non-polar solvents including H₂O, MeOH, EtOH, CH₃CN, CHCl₃, DMSO and DMF was tested and the results showed the stability of complexes in solvents. The most characteristic feature in the IR spectra of the ligands comes from the C=N stretching vibrations. This band appeared at 1625, 1629, 1623 and 1627 cm⁻¹ for **Cl₂LH**, **Br₂LH**, **I₂LH** and **BrCILH**, respectively [36].

Compared to the free Schiff base ligands, this band was shifted to lower wavenumber upon coordination (1619, 1618, 1616 and 1619 cm⁻¹ for **(Cl₂L)₂Cu**, **(Br₂L)₂Cu**, **(I₂L)₂Cu** and **(BrCIL)₂Cu**, respectively) [37]. Formation of M-N bonds leads to weakening of C=N band and this can be explained by the donation of electrons from the nitrogen atom to the empty orbitals of the metal atom. Additional support for the formation of the complexes were provided by the existence of weak intensity bands at ~ 480 cm⁻¹ and ~ 520 cm⁻¹ attributed to the formation of M-N and M-O bonds, respectively.

The ¹H NMR and ¹³C NMR spectra of the Schiff base ligands, **Cl₂LH**, **Br₂LH**, **I₂LH** and **BrCILH** were measured in CDCl₃, with TMS as internal standard. The data is depicted in experimental section and spectra in Figs. S1-S7 and ¹H NMR of **I₂LH** in Fig. 3. The ¹H and ¹³C NMR spectra of all ligands obtained after 12, 24 and 120 h were similar to the initial spectrum, indicating that the ligands are stable in deuterated chloroform. The ¹H NMR spectra of all ligands show one peak as triplet at ~ 8.2 ppm corresponding to the imine proton (CH=N), and a sharp O—H signal at ~14.5 ppm (for example see the ¹H NMR spectrum of **I₂LH** in Fig. 3). The very sharp peak for the phenolic (-OH) proton in the prepared Schiff bases can be ascribed to the

intramolecular hydrogen-bonding interaction of this functional group with nitrogen heteroatom of imine functionality. The ^1H NMR spectra also show a multiplet peak for $-\text{CH}-\text{CH}=\text{CH}_2$ proton at ~ 6.0 ppm. The reason for splitting of $-\text{CH}$ peak is coupling of hydrogen of $-\text{CH}$ with $-\text{CH}_2$ and $=\text{CH}$ hydrogens.

3.2. X-ray Crystal Structure

The molecular structures of all complexes were determined by single crystal X-ray diffraction technique. View of the molecular structures of $(\text{Cl}_2\text{L})_2\text{Cu}$, $(\text{Br}_2\text{L})_2\text{Cu}$, $(\text{I}_2\text{L})_2\text{Cu}$ and $(\text{BrCIL})_2\text{Cu}$ complexes with common atom numbering scheme are shown in Fig. 4. Crystallographic data and selected bond distances and angles of complexes are listed in Tables 1 and 2, respectively. Single crystal X-ray analysis reveals all complexes crystallize in centrosymmetric space groups (monoclinic $\text{P}2_1/\text{c}$ for $(\text{Br}_2\text{L})_2\text{Cu}$, $(\text{I}_2\text{L})_2\text{Cu}$ and $(\text{BrCIL})_2\text{Cu}$; triclinic $\text{P}-1$ for $(\text{Cl}_2\text{L})_2\text{Cu}$). The crystallographic data also reveal that in all complexes the metal center is four coordinated by two phenolate oxygen and two imine nitrogen atoms of two moles of Schiff base ligand. The coordination geometry around the $\text{Cu}(\text{II})$ in all reported compounds is best described as square planar with two axially elongated interactions named metal-halogen secondary bonds ($\text{Cu}\cdots\text{X}$).

Examination of the main metal-ligand distances in all complexes, Table 2, shows that the $\text{Cu}-\text{N}$ distances are longer than the $\text{Cu}-\text{O}$ distances due to stronger ability of the oxygen atom to bond to the metal than the nitrogen atom [38,39]. The $\text{Cu}-\text{N}$ distances are 2.0002(3), 2.0002(3), 2.019(8) and 2.007(2) Å, while, the $\text{Cu}-\text{O}$ distances are 1.895(2), 1.901(2), 1.919(7) and 1.9055(17) Å for $(\text{Cl}_2\text{L})_2\text{Cu}$, $(\text{Br}_2\text{L})_2\text{Cu}$, $(\text{I}_2\text{L})_2\text{Cu}$ and $(\text{BrCIL})_2\text{Cu}$, respectively. These bond lengths ($\text{Cu}-\text{O}$ and $\text{Cu}-\text{N}$) and bond angles ($\text{N}-\text{Cu}-\text{O}$) (Table 2) are similar to those seen in

related complexes [17,40,41]. For instance, in our previous work, distances of 1.902(2) and 1.896(2) Å for the Cu—O bond and 2.014(3) and 2.003(3) Å for Cu—N bond and angles of 88.14(13) and 88.44(12) for N—Cu—O are found in a copper(II) complex derived from salicylaldehyde and allylamine [21].

As shown in Figs. 5-8, there are halogen-halogen type I interactions in all of the complexes. A statistical study proved that at distances inferior to the sum of van der Waals radii type I interactions are dominant, while at distances close to the value of that sum halogen bonds prevail. However, when the contact distance is superior to the van der Waals radii sum, type I becomes more frequent, particularly for I...I contacts [42].

As we can see for $(\text{Cl}_2\text{L})_2\text{Cu}$ in Fig. 5, only halogens in *para* position (Cl_2) can involve in intermolecular halogen-halogen interaction. The $\text{Cl}_2\dots\text{Cl}_2$ interaction length is 3.5639 Å that is little more than the sum of van der Waals radii (3.52 Å) (Table 3). In the $(\text{Br}_2\text{L})_2\text{Cu}$ and $(\text{I}_2\text{L})_2\text{Cu}$, the halogen atom in the *ortho* position (X_1) also involve in halogen-halogen interaction with *para* halogen of another molecule with $\text{Br}_1\dots\text{Br}_2$ distance of 3.8922 Å for $(\text{Br}_2\text{L})_2\text{Cu}$ and with $\text{I}_1\dots\text{I}_2$ distance of 4.0633 Å for $(\text{I}_2\text{L})_2\text{Cu}$ (Figs. 6 and 7 and Table 3). Then, in $(\text{Br}_2\text{L})_2\text{Cu}$ and $(\text{I}_2\text{L})_2\text{Cu}$ complexes, each *para*-halogen (Br or I) acts as both halogen bond donor and an acceptor in the generation of bifurcated $\text{X}\dots\text{X}$ halogen bonding interactions. The *para*-halogen-*para*-halogen interaction for $\text{Cl}\dots\text{Cl}$ in $(\text{Cl}_2\text{L})_2\text{Cu}$ is 3.5639, for $\text{Br}\dots\text{Br}$ in $(\text{Br}_2\text{L})_2\text{Cu}$ is 3.8610 Å and for $\text{I}\dots\text{I}$ in $(\text{I}_2\text{L})_2\text{Cu}$ is 3.8260 Å. These $\text{X}\dots\text{X}$ contacts, except one $\text{I}\dots\text{I}$ in $(\text{I}_2\text{L})_2\text{Cu}$, are just a little longer than the sum of Bondi's van der Waals radii of halogens (Table 3). The vdW radii for Cl, Br, and I atoms are 1.76, 1.87, and 2.03 Å, respectively, and the corresponding sum of the vdW radii are $\text{Cl} + \text{Cl} = 3.52$; $\text{Br} + \text{Br} = 3.74$ and $\text{I} + \text{I} = 4.06$ Å. In $(\text{BrClI})_2\text{Cu}$ complex, only Br in *ortho*-position have a very weak interaction with the chlorine atom of neighbor

molecule. The distance for this weak halogen-halogen interaction is 3.91 Å. This should be noted that the vdW radii for Cl and Br atoms are 1.76 and 1.87 Å, respectively, and the corresponding sum of the vdW radii is $\text{Cl} + \text{Br} = 3.63$ Å.

Another interesting interaction in these complexes is metal-halogen secondary bonds. As shown in Figs. 5-8, two axial directions of Cu atom occupied by two *para*-halogen atoms of two different complexes. The closest separation is 3.421 Å for Cu...Cl in $(\text{Cl}_2\text{L})_2\text{Cu}$, 3.463 Å for Cu...Br in $(\text{Br}_2\text{L})_2\text{Cu}$ and 3.486 Å for Cu...I in $(\text{I}_2\text{L})_2\text{Cu}$. For comparison, the sum of the Bondi's van der Waals radii of copper with chlorine, bromine and iodine are 3.16 (1.40 + 1.76), 3.27 (1.40 + 1.87) and 3.43 (1.40 + 2.03) Å, respectively. In the complex $(\text{BrClI})_2\text{Cu}$, *para*-chlorine atoms have interaction with Cu with Cu...Cl distance of 3.467 Å. The Cu-Halogen- C_{phen} angle is 92.26(13), 92.26(13), 92.26(13) and 92.26(13)° in $(\text{Cl}_2\text{L})_2\text{Cu}$, $(\text{Br}_2\text{L})_2\text{Cu}$, $(\text{I}_2\text{L})_2\text{Cu}$ and $(\text{BrClI})_2\text{Cu}$ complexes, respectively, which is close to the expected angle of 90° that would ideally position the region of negative electrostatic potential on the halogen atom to interact with the metal center. Hence, we can say in all reported complexes, the coordination geometry around the Cu(II) can be described in best way as square planar plus two axially elongated interactions.

Interaction between terminal hydrogen of allyl group ($\text{RHC}=\text{CHH}$) with one carbon atom of benzene group of the nearest neighbor molecule is another interesting intermolecular interaction in these complexes. The terminal H atoms in Allyl group attached to C_{sp^2} and for this reason is approximately positive. These positive hydrogen atoms can have interaction with π system of benzene group of neighbor molecule (Fig. 9). This interaction involves the atom of H(10B) pointing directly to the system π C1-C2 in $(\text{Cl}_2\text{L})_2\text{Cu}$ with distance of 2.898 and 3.112 Å, and

H(10A) to the system π C1-C2 with distance of 2.905 and 2.966 Å in **(Br₂L)₂Cu**, 3.053 and 3.182 Å in **(I₂L)₂Cu** and 2.870 and 2.877 Å in **(BrCIL)₂Cu**.

In the all complexes, the $-\text{CH}=\text{CH}_2$ group is almost perpendicular to plane of molecule. The angle between created plane of N1-O1-Cu1-O1'-N1' atoms and N1-C8-C9 atoms is 92.26(13), 92.26(13), 92.26(13) and 92.26(13)° in **(Cl₂L)₂Cu**, **(Br₂L)₂Cu**, **(I₂L)₂Cu** and **(BrCIL)₂Cu** complexes, respectively. This arrangement allows to the $-\text{N}-\text{CH}_2$ and $-\text{N}-\text{CH}_2-\text{CH}$ hydrogen atoms having suitable intramolecular interaction with oxygen atom (Fig. 10). We saw this kind of arrangement of allyl group also in our previous work in preparation of Cu(II), Co(II) and Zn(II) complexes from salicylaldehyde and allylamine [21]. These two intramolecular interactions can be described as $S^1_2(5)$ [43].

Another important intermolecular interaction in these complexes is $\pi\dots\pi$ interactions. As shown in Table 4 and Scheme 4, $\pi\dots\pi$ interactions exist between Cg(1)...Cg(2) with centroid-centroid distance of 3.6502 and 3.5273 Å for **(Cl₂L)₂Cu**, 3.6593 and 3.5870 Å for **(Br₂L)₂Cu**, 3.7488 and 3.5638 Å for **(I₂L)₂Cu** and 3.6465 and 3.5918 Å for **(BrCIL)₂Cu** in which Cg(1) and Cg(2) are centers of Cu(1)/O(1)/C(1)/C(6)/C(7)/N(1) and C(1)/C(6) rings, respectively.

3.3. Hirshfeld surface analysis

Hirshfeld surface (HS) based tools represent a unique approach to the crystal structure prediction and this method offers a facile way of obtaining information on trends in crystal packing [34]. Hirshfeld surfaces and their associated finger print plots for synthesized complexes were calculated using *CrystalExplorer 3.1* and are illustrated in Figs. 11 and 12 [33,35]. The distances from the Hirshfeld surface to the nearest atoms outside and inside the surface are the quantities d_e and d_i , respectively, and the normalized contact distance based on these, $d_{\text{norm}} = (d_i -$

$r_i^{\text{vdw}}/r_i^{\text{vdw}}+(d_e-r_e^{\text{vdw}})/r_e^{\text{vdw}}$, is symmetric in d_e and d_i , with d_i^{vdw} and d_e^{vdw} being the van der Waals radii of the atoms. The mapping of d_{norm} on the Hirshfeld surface highlights the donor and acceptor equally and it is a powerful tool for analyzing directional intermolecular interactions, as it displays a surface where contacts shorter than the sum of their van der Waals radii have negative values of d_{norm} and appear as conspicuous red spots; contacts longer than the van der Waals distances have positive values of d_{norm} and are mapped in blue. Hirshfeld surface of synthesized copper complexes bear a lot of similarities (due to similar structure of the complex compounds) and will be therefore described together.

According to the Hirshfeld surface analysis, Fig. 13, for all four complexes, the intermolecular Hal...H contacts, comprising 31.6 (Cl...H), 30.5 (Br...H), 31.4 (I...H) and 31.1% (for both Cl...H and Br...H) of the total number of contacts for **(Cl₂L)₂Cu**, **(Br₂L)₂Cu**, **(I₂L)₂Cu** and **(BrCIL)₂Cu** respectively, are major contributors to the crystal packing. The shortest H...Hal contacts are shown on the fingerprint plots as a pair of spikes at $d_e + d_i \approx 2.8$ Å for **(Cl₂L)₂Cu**, ~ 3.0 Å for **(Br₂L)₂Cu**, ~ 3.1 Å for **(I₂L)₂Cu** and ~ 3.1 - 3.2 Å for **(BrCIL)₂Cu** (Fig. 12).

According to the Hirshfeld surface analysis also intermolecular H...H contacts, comprising ~ 29 % of the total number of contacts, are one of major contributors to the crystal packing (Fig. 13). As shown in Fig. 12, the shortest H...H contacts in the fingerprint plots of all complexes are at $d_e + d_i = 2.3$ – 2.5 Å. The H...H contacts are characterized by broader spikes in **(Cl₂L)₂Cu** and **(BrCIL)₂Cu** and relatively sharper spikes in **(Br₂L)₂Cu**. Furthermore, a subtle feature, splitting in the fingerprint plots of H...H, is evident in the fingerprint plot of **(I₂L)₂Cu**. This splitting occurs when the shortest contact is between three atoms, rather than for a direct two-atom contact.

The C...C contacts are shown on the fingerprint plots of all complexes as the characteristic pale blue/green, mixed with yellow points, area on the diagonal at $d_e = d_i \approx 1.7\text{--}2.1$ Å (Fig. 12), and attributed to the formation of the above mentioned strong $\pi\cdots\pi$ stacking interactions (Table 4). However, this $\pi\cdots\pi$ stacking interactions is less than 6% of the total Hirshfeld surface area of complexes.

The fingerprint plots of all copper complexes features spike of various lengths and thickness, and the most prominent being the presence of wing- like peripheral spikes for C...H contact at the top left and bottom right of each plot (Fig. 12). The spike at the top left corresponds to the points on the surface around the C–H donor, while those at the bottom right correspond to the surface around the π acceptor [44]. As shown in Fig 3, the shortest C...H distance ($d_e + d_i$) is $\approx 2.8\text{--}2.9$ Å. The most important C–H... π interaction in the packing of all copper complexes is related to interaction of hydrogen of allyl group (RHC=CHH) with one carbon of benzene group of the nearest neighbor molecule. Hirshfeld surface analysis show this short interaction as red spot (Fig. 11). For the **(BrCIL)₂Cu**, we can see two red spots for this interaction. This splitting occurs when the shortest contact is between three atoms, rather than for a direct two-atom contact. As shown in Fig 11, the hydrogen of ally group (H10A) in complex **(BrCIL)₂Cu** have short interaction with C1 and C6 of benzene group of the nearest neighbor molecule.

It is worth to mention that, the molecular surface of **(Cl₂L)₂Cu** and **(BrCIL)₂Cu** complexes is also populated by Hal...N contact (2.1%) and C...O contacts (1.9 and 2.3% for **(Cl₂L)₂Cu**, and **(BrCIL)₂Cu**, respectively). The contribution of C...O contacts for **(Br₂L)₂Cu** and **(I₂L)₂Cu** is 2.1 and 1.7%, respectively.

Close inspection of other intermolecular contacts in the structures of all copper complexes also revealed a negligible proportion of Cu...C (0.2–0.3%), Cu...H (0.1–0.2%), Hal...O (0.7–1.4%), C...N (0.3–0.4%), O...H (0.6–1.2%) and N...H (1.2–1.3%) (Fig. 13).

3.4. Theoretical calculations

As can be seen in Fig. S8, the four compounds are all engaged in a series of intermolecular interactions that determine the whole molecular packing. Three of the four complexes are isomorphic while the fourth: $(\text{Cl}_2\text{L})_2\text{Cu}$, it crystallizes in the P-1 space group with a halved cell volume with respect to others.

Compound $(\text{Cl}_2\text{L})_2\text{Cu}$ is the only compound that, thanks to Cl...Cl and H...Cl interactions, it forms a series of 2D supramolecular aggregates that extend according to the (-424) crystallographic plans as depicted in Fig. 14. The chlorine-chlorine interaction makes an angle C-Cl ... Cl of 152.63° and a Cl...Cl distance of 3.5639 \AA , just above the sum of van der Waals radii (3.52 \AA), although is not in the optimal geometry that provides an interaction between the negative belt and the positive hole at 90° . However, is an interaction which brings a positive contribution ($0.42 \text{ kcal mol}^{-1}$) to the overall reticular energy (See Fig. S9 and S10). The same halogen-halogen interaction is present in the $(\text{I}_2\text{L})_2\text{Cu}$ and $(\text{Br}_2\text{L})_2\text{Cu}$ compounds. The geometry of the interaction is almost the same as that observed with the chlorine compound, with the interaction energy of 0.65 and $0.56 \text{ kcal mol}^{-1}$ for $(\text{I}_2\text{L})_2\text{Cu}$ and $(\text{Br}_2\text{L})_2\text{Cu}$, respectively. (Fig. S10).

Also, all the complexes show metal-halogen interaction along with π - π stacking interaction that leads to a head to tail coupling between two centrosymmetric compounds. The range of energy is from $6.04 \text{ kcal mol}^{-1}$ for $(\text{Br}_2\text{L})_2\text{Cu}$, until $7.94 \text{ kcal mol}^{-1}$ for $(\text{Cl}_2\text{L})_2\text{Cu}$ as reported in Fig. 15.

The Cu...X separations are all in a narrow range: 3.421 Å ((Cl₂L)₂Cu); 3.467 Å ((BrCIL)₂Cu); 3.463 Å ((Br₂L)₂Cu) and 3.486 Å for iodine compound (I₂L)₂Cu. All separations are slightly above the sum of the van der Waals radii. The interaction can arise from a strong connection between the halogen lone pair (HOMO's) and the empty 4pz orbital of copper atoms, metal-halogen interactions as depicted in Fig. 16 where the three involved MO from single monomers are pictorially put together.

There is a HB- π interaction involving the terminal hydrogen atom of the ethylenic fragment and the phenyl ring in all four complexes. This interaction involves the atom of H(10B) pointing directly to the system π C1-C2 with distance of 2.898 and 3.112 Å for (Cl₂L)₂Cu and atom H(10A) to the system π C1-C2 for (Br₂L)₂Cu with distance of 2.905 and 2.966 Å, for (BrCIL)₂Cu with distance of 2.870 and 2.877 Å and for (I₂L)₂Cu with distance of 3.053 and 3.182 Å. These interactions, whose energy diagrams are depicted in Fig. 17, contributes significantly to molecular packing with an energy that varies from a minimum of 2.05 kcal mol⁻¹ in (Cl₂L)₂Cu to a maximum of 3.15 kcal mol⁻¹ in the complex (I₂L)₂Cu. For the two remaining compounds, it has the value of 2.61 and 2.62 kcal mol⁻¹ for (Br₂L)₂Cu and (BrCIL)₂Cu, respectively. Last attractive interaction is observed in the compounds (BrCIL)₂Cu and (I₂L)₂Cu (Fig. 18), in it the halogen atoms I₁ and Br₁ point towards the π system of the phenyl ring. In the solid state the two distances are just below the sum of the van der Waals radii (I...C3: 3.627 Å (3.680 Å) and Br...C3: 3.567 Å (3.670 Å)). The computed energies show minimum energy of 0.66 and 0.55 kcal mol⁻¹ for (BrCIL)₂Cu and (I₂L)₂Cu, respectively. The low energy for both interactions depends on the non-perfect geometry of this kind of interaction (C-I...C3 153.73° and C-Br...C3 158.35°).

Generally, minimum energy distance computed with SPE procedure don't correspond to the distance found at experimental observed position in the solid state. This is because in the solid state the crystallographic minimum energy results from a suitable balance of all attractive and repulsive interactions. While with the calculation we explore a single interaction, at most, as in the case of metal halogen interaction and π - π staking are two interactions that determine the total energy.

4. Conclusions

To summarize, we have presented the preparation, structural and computational analysis of four new Cu(II) coordination compounds based on new halogenated Schiff base ligands derived from halogenated salicylaldehydes (3,5-dichlorosalicylaldehyde, 3,5-dibromosalicylaldehyde, 3,5-diiodosalicylaldehyde and 3-bromo-5-chlorosalicylaldehyde) and allyl amine. All complexes show halogen-halogen of type I, π - π , CH- π interactions and also metal-halogen secondary bonds in crystal packing. The coordination geometry around the Cu(II) in all reported compounds is best described as square planar plus two axially elongated interactions (Cu...X) named metal-halogen secondary bonds. According to the Hirshfeld surface analysis, the intermolecular Hal...H and H...H and C...H contacts, are major contributors in the crystal packing. Also, all of the interactions in crystal packing have been analyzed by theoretical calculations.

Appendix A. Supplementary data

CCDC 1839638, 1839639, 1839640 and 1839641 contain the supplementary crystallographic data for **(BrCl₂L)₂Cu**, **(Br₂L)₂Cu**, **(I₂L)₂Cu** and **(Cl₂L)₂Cu**, respectively. These data can be

obtained free of charge via <http://www.ccdc.cam.ac.uk/conts/retrieving.html>, or from the Cambridge Crystallographic Data Centre, 12 Union Road, Cambridge CB2 1EZ, UK. Fax: +44 1223 336 033; or e-mail: deposit@ccdc.cam.ac.uk

Acknowledgements

The authors are grateful to the Research Council of the University of Isfahan for financial support of this work and also university of Messina for determination of structures by SCXRD instrument.

References

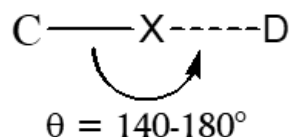
- [1] G. Cavallo, P. Metrangolo, T. Pilati, G. Resnati and G. Terraneo, *Cryst. Growth Des.*, 14 (2014) 2697.
- [2] G. Cavallo, P. Metrangolo, R. Milani, T. Pilati, A. Priimagi, G. Resnati and G. Terraneo, *Chem. Rev.*, 116 (2016) 2478.
- [3] P. Metrangolo and G. Resnati, *Halogen Bonding. Fundamentals and Applications*, Springer-Verlag: Berlin, Heidelberg, 2008.
- [4] A. Mukherjee, S. Tothadi, and G. R. Desiraju, *Acc. Chem. Res.*, 47 (2014) 2514.
- [5] B. K. Saha, A. Saha and S. A. Rather, *Cryst. Growth Des.*, 17 (2017) 2314.
- [6] M. H. Kolar and P. Hobza, *Chem. Rev.*, 116 (2016) 5155.
- [7] S. K. Nayak, M. K. Reddy, T.N. Guru Row and D. Chopra, *Cryst. Growth Des.*, 11 (2011) 1578.

- [8] B. K. Saha, A. Nangia and J-F. Nicoud, *Cryst. Growth Des.*, 4 (2004) 279.
- [9] J. S. Murray, L. Macaveiu and P. J. Politzer, *Comput. Sci.*, 5 (2014) 590.
- [10] P. Politzer, J. S. Murray and T. Clark, *Phys. Chem. Chem. Phys.*, 15 (2013) 11178.
- [11] L. C. Gilday, S. W. Robinson, T. A. Barendt, M. J. Langton, B. R. Mullaney, and P. D. Beer, *Chem. Rev.*, 115 (2015) 7118.
- [12] D. Schollmeyer, O. V. Shishkin, T. Rühl and M. O. Vysotsky, *CrystEngComm.*, 10 (2008) 715.
- [13] T. E. Machonkin, M. D. Boshart, J. A. Schofield, M. M. Rodriguez, K. Grubel, D. Rokhsana, W. W. Brennessel and P. L. Holland, *Inorg. Chem.*, 53 (2014) 9837.
- [14] S. S. Rocks, W. W. Brennessel, T. E. Machonkin and P. L. Holland, *Inorg. Chem.*, 49 (2010) 10914.
- [15] J. A. Schofield, W. W. Brennessel, E. Urnezius, D. Rokhsana, M. D. Boshart, D. H. Juers, P. L. Holland and T. E. Machonkin, *Eur. J. Inorg. Chem.*, (2015) 4643.
- [16] M. F. Richardson, G. Wulfsberg, R. Marlow, S. Zaghonni, D. McCorkle, K. Shadid, J. Gagliardi Jr and B. Farris, *Inorg. Chem.*, 32 (1993) 1913.
- [17] N. Poulter, M. Donaldson, G. Mulley, L. Duque, N. Waterfield, A.G. Shard, S. Spencer, A. Tobias, A. Jenkins and A.L. Johnson, *New J. Chem.*, 35 (2011) 1477.
- [18] S. Majumder, A. Bhattacharya, J.P. Naskar, P. Mitra and S. Chowdhury, *Inorg. Chim. Acta.*, 399 (2013) 166.
- [19] Z. Kazemi, H. Amiri Rudbari, M. Sahihi, V. Mirkhani, M. Moghadam, S. Tangestaninejad, I. Mohammadpoor-Baltork and S. Gharaghani, *J. Photochem. Photobiol. A.*, 162 (2016) 448.

- [20] H. Amiri Rudbari, M. Khorshidifard, B. Askari, N. Habibi and G. Bruno, *Polyhedron.*, 100 (2015) 180.
- [21] M. Khorshidifard, H. Amiri Rudbari, Z. Kazemi-Delikani, V. Mirkhani and R. Azadbakht, *J. Mol. Struct.*, 1081 (2015) 494.
- [22] H. Amiri Rudbari, M.R. Iravani, V. Moazam, B. Askari, M. Khorshidifard, N. Habibi and G. Bruno, *J. Mol. Struct.*, 1125 (2016) 113.
- [23] (a) COSMO, version 1.60, Bruker AXS Inc., Madison, Wisconsin, (2005).; (b) SAINT, version 7.06A, Bruker AXS Inc., Madison, Wisconsin, (2005).; (c) SADABS, version 2.10, Bruker AXS Inc., Madison, Wisconsin, (2005).
- [24] M.C. Burla, R. Caliandro, M. Camalli, B. Carrozzini, G.L. Cascarano, L. De Caro, C. Giacovazzo, G. Polidori and R. Spagna, *J. Appl. Crystallogr.*, 38 (2005) 381.
- [25] G.M. Sheldrick, *SHELXL-97*, University of Göttingen, Göttingen, Germany, (1997).
- [26] Frisch, M. J. et al. *Gaussian 09*, Revision D.01. *Gaussian 09W*, Revision D.01, Gaussian, Inc., Wallingford CT (2009).
- [27] A.D. Becke, *J. Chem. Phys.*, 98 (1993) 5648.
- [28] D. Andrae, U. Haeussermann, M. Dolg, H. Stoll and H. Preuss, *Theoretica chimica acta*, 77 (1990) 123.
- [29] J. Heyd, G.E. Scuseria and M. Ernzerhof, *J. Chem. Phys.*, 124 (2006) 219906.
- [30] J.P. Perdew, K. Burke and M. Ernzerhof, *Phys. Rev. Lett.*, 77 (1996) 3865.
- [31] F.A. Hamprecht, A.J. Cohen, D.J. Tozer and N.C. Handy, *J. Chem. Phys.*, 109 (1998) 6264.
- [32] S. F. Boys and F. Bernardi, *Mol. Phys.*, 19 (1970) 553.
- [33] S. K. Wolff, D. J. Grimwood, J. J. McKinnon, M. J. Turner, D. Jayatilaka and M. A. Spackman, *CrystalExplorer* (Version 3.1), University of Western, Australia., (2012).

- [34] M. A. Spackman and D. Jayatilaka, *CrystEngComm.*, 11 (2009) 19.
- [35] M. A. Spackman and J. J. McKinnon, *CrystEngComm.*, 4 (2002) 378.
- [36] M. Dehkhodaei, M. Khorshidifard, H. Amiri Rudbari, M. Sahihi, G. Azimi, N. Habibi, S. Taheri, G. Bruno and R. Azadbakht, *Inorg. Chim. Acta.*, 466 (2017) 48.
- [37] Z. Kazemi, H. Amiri Rudbari, V. Mirkhani, M. Sahihi, M. Moghadam, S. Tangestaninejad, I. Mohammadpoor-Baltork, A.A. Kajani and G. Azimi, *Eur. J. Med. Chem.*, 135 (2017) 230.
- [38] P. K. Bhaumik, A. Bauzá, M. G. B. Drew, A. Frontera and S. Chattopadhyay, *CrystEngComm.*, 17 (2015) 5664.
- [39] E. Loukopoulos, B. Berkoff, K. Griffiths, V. Keeble, V. N. Dokorou, A. C. Tsipis, A. Escuer and G. E. Kostakis, *CrystEngComm.*, 17 (2015) 6753.
- [40] M. Enamullah, A. K. M. R. Uddin, G. Pescitelli, R. Berardozzi, G. Makhloufi, V. Vasylyeva, A-C. Chamayou and C. Janiak, *Dalton Trans.*, 43 (2014) 3313.
- [41] M. Enamullah, M. A. Islam, B. A. Joy, G. J. Reiss, *Inorg. Chim. Acta.*, 453 (2016) 202.
- [42] J. L. Ferreira da Silva, K. Shimizu and M. T. Duarte, *CrystEngComm.*, 19 (2017) 2802.
- [43] J. Bernstein, R.E. Davis, L. Shimoni and N.-L. Chang, *Angew. Chem., Int. Ed. Engl.*, 34 (1995) 1555.
- [44] R. Soman, S. Sujatha and C. Arunkumar, *J. Fluorine Chem.*, 163 (2014) 16.

a) Halogen Bonding



X (acceptor) = Cl, Br, I

Electrophilic species

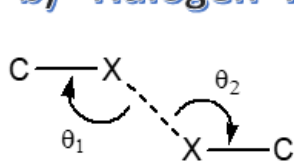
(Lewis acid)

D (donor) = O, N, S, Se

lone pair-possessing species

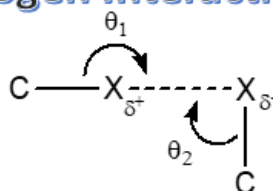
(Lewis base)

b) Halogen–Halogen Interactions



$$\theta_1 = \theta_2 = 140 \sim 180^\circ$$

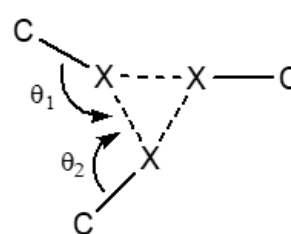
Type I



$$\theta_1 = 150 - 180^\circ$$

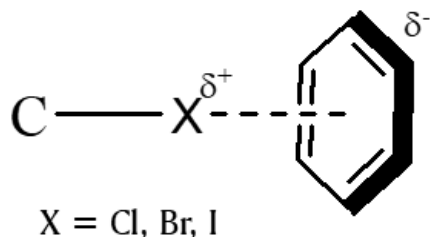
$$\theta_2 = 90 - 120^\circ$$

Type II

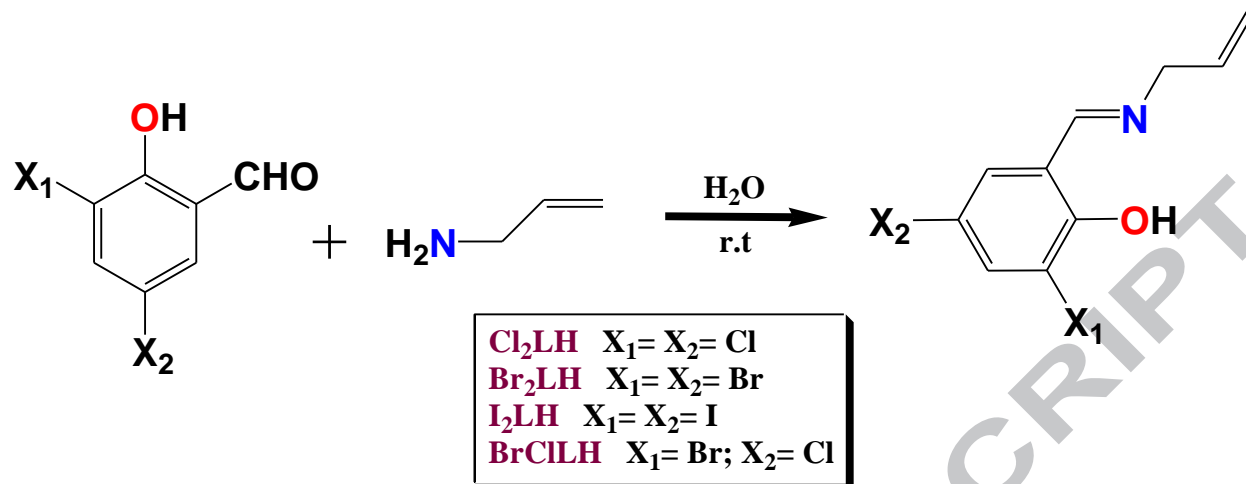


X = Cl, Br, I

X₃ synthon

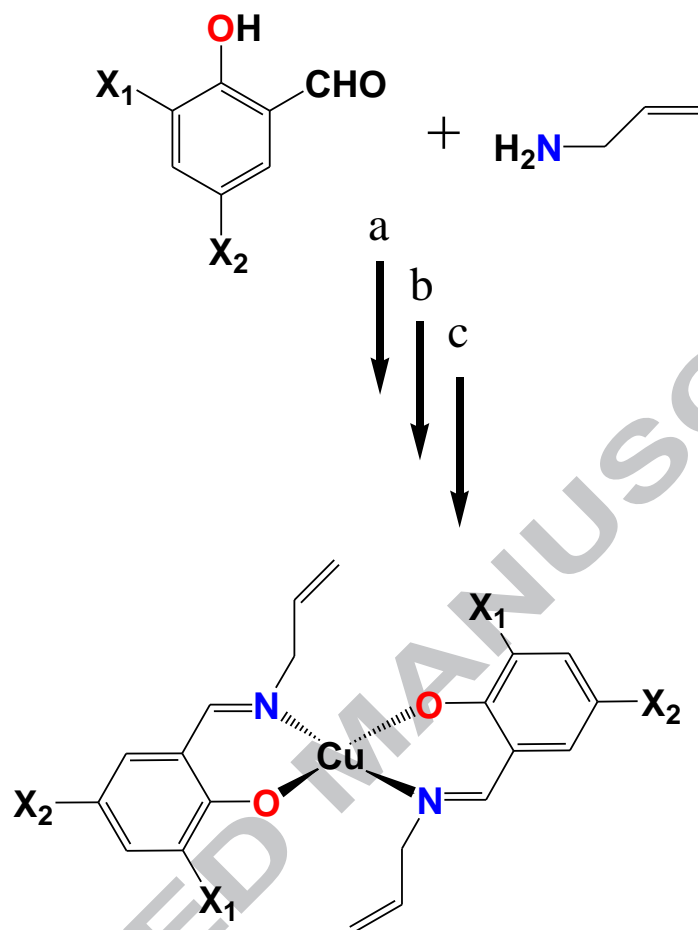
c) Halogen– π Interactions

Scheme 1 Schematic representations of three intermolecular halogen interactions, halogen bonding, halogen-halogen interaction, halogen- π interaction.

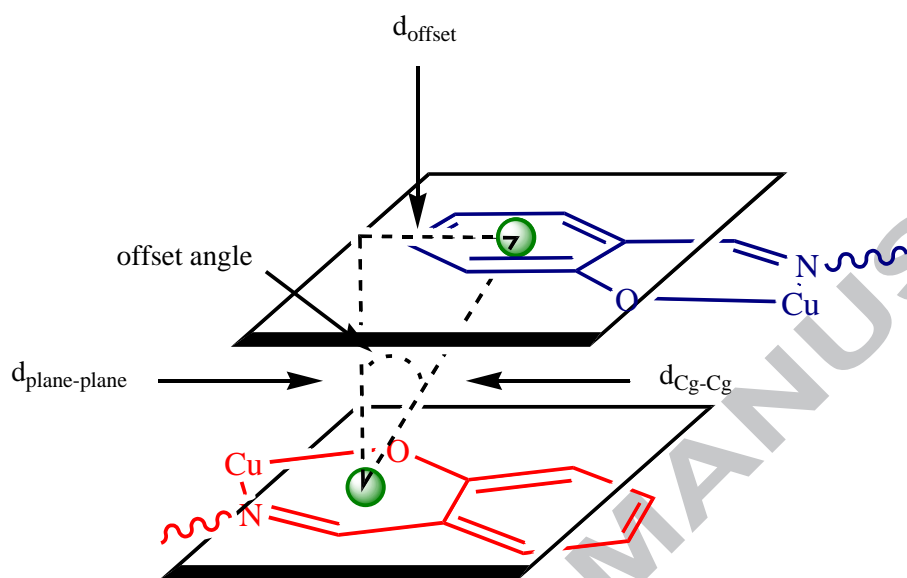


Scheme 2 Preparation of ligands

ACCEPTED MANUSCRIPT



Scheme 3 Synthetic routes for the preparation of the complexes: (a) stirring of allylamine and halogenated salicylaldehydes (3,5-dichlorosalicylaldehyde, 3,5-dibromosalicylaldehyde, 3,5-diiodosalicylaldehyde, 3-Bromo-5-chlorosalicylaldehyde) in MeOH at ambient temperature; (b) adding of trimethylamine to solution and stirring for 10 minutes; (c) adding of CuCl₂ and stirring in ambient temperature and then reflux for 3 hours (X₁=X₂=Cl in (Cl₂L)₂Cu; X₁=X₂=Br in (Br₂L)₂Cu; X₁=X₂=I in (I₂L)₂Cu and X₁= Br, X₂=Cl in (BrClL)₂Cu).



Scheme 4. Schematic representation of geometrical parameters for definition of π - π stacking

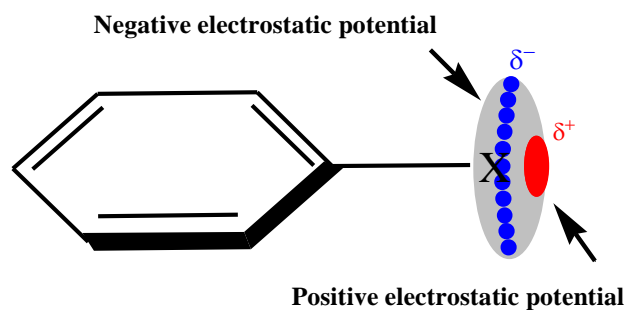


Fig. 1 Regions of positive and negative electrostatic potential highlighting the anisotropy associated with the electron density distribution around the covalently bonded X (halogen) atom.

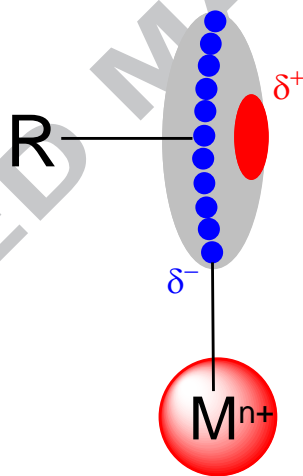


Fig. 2 Illustration of the type of anisotropic charge distribution found for polarizable halogen atoms, which can lead to metal–halogen secondary bonding.

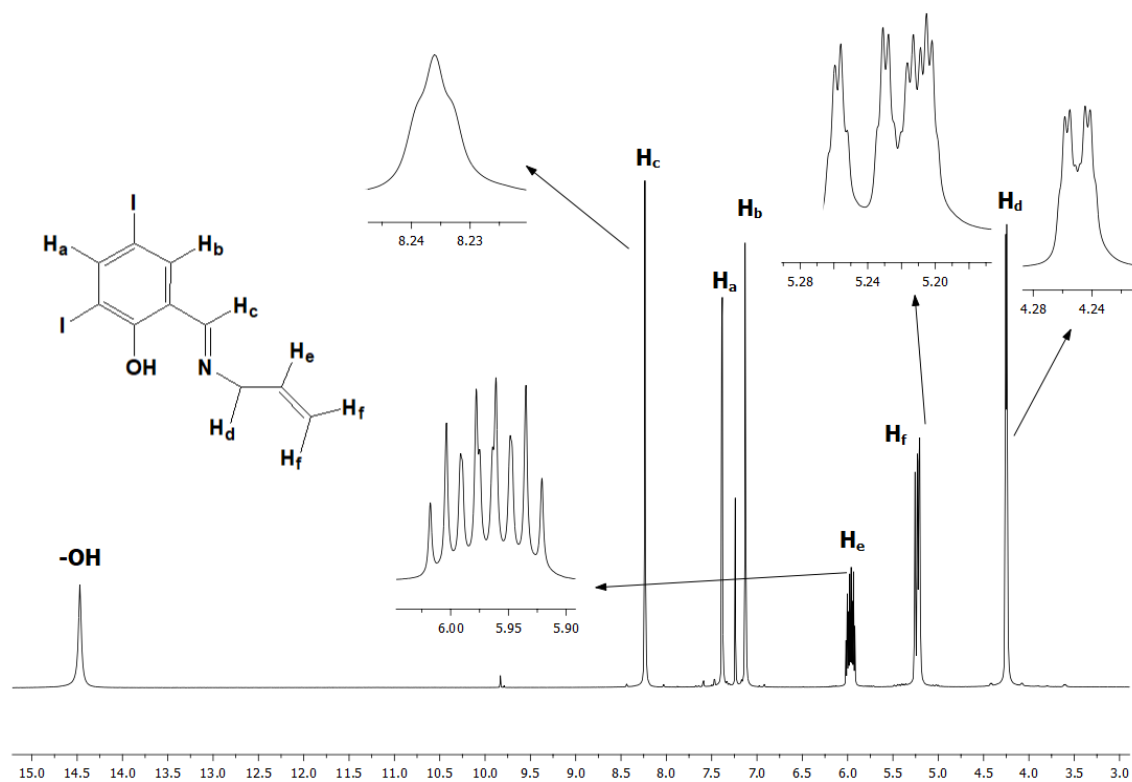


Fig. 3 ^1H NMR spectrum of I_2LH

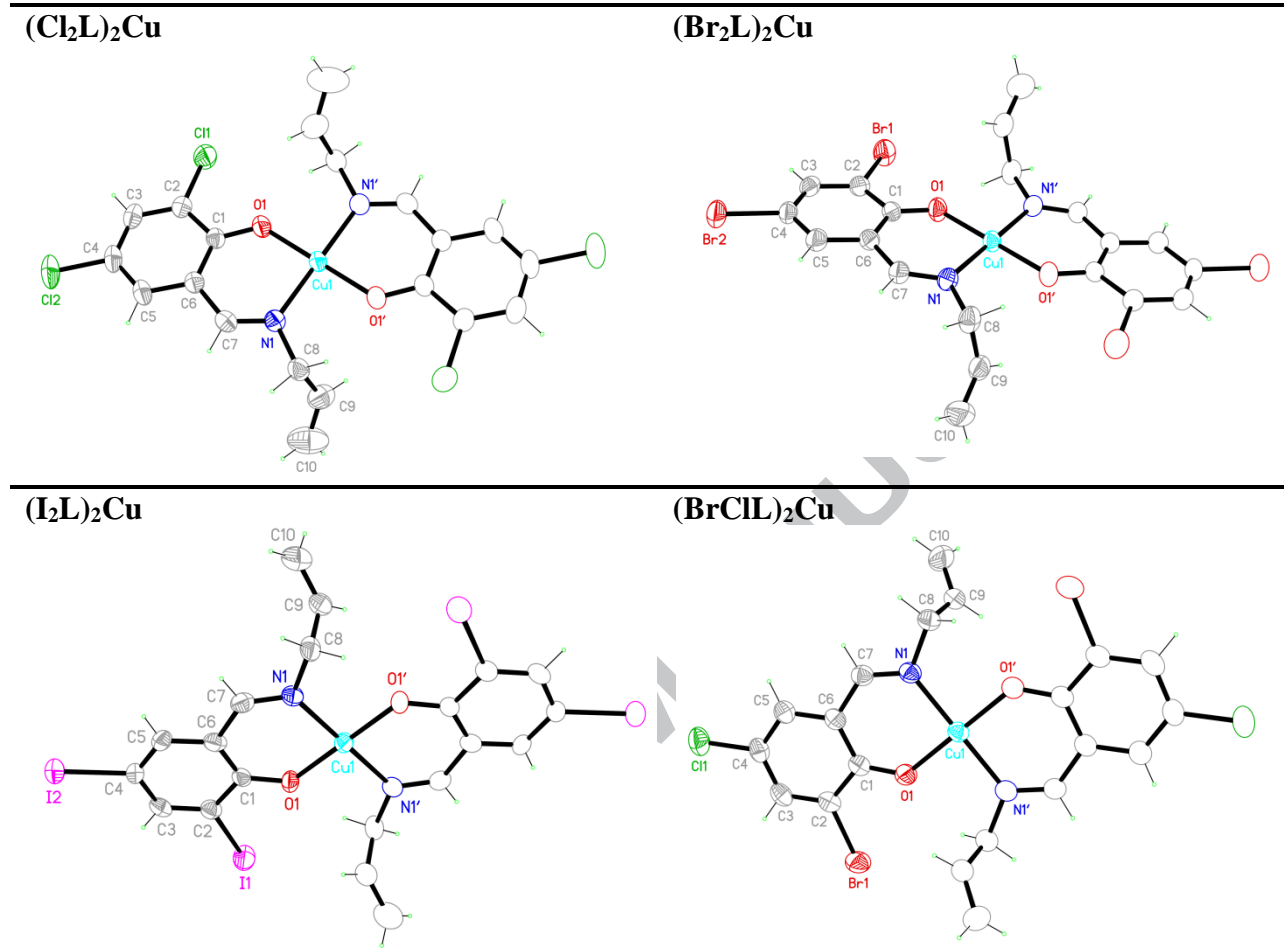


Fig. 4 Perspective view of copper complexes constituted by the asymmetric unit (filled drawings) showing the numbering scheme and the centrosymmetric half part (empty drawings). Thermal ellipsoids are drawn at the 50% probability level, while the hydrogen size is arbitrary.

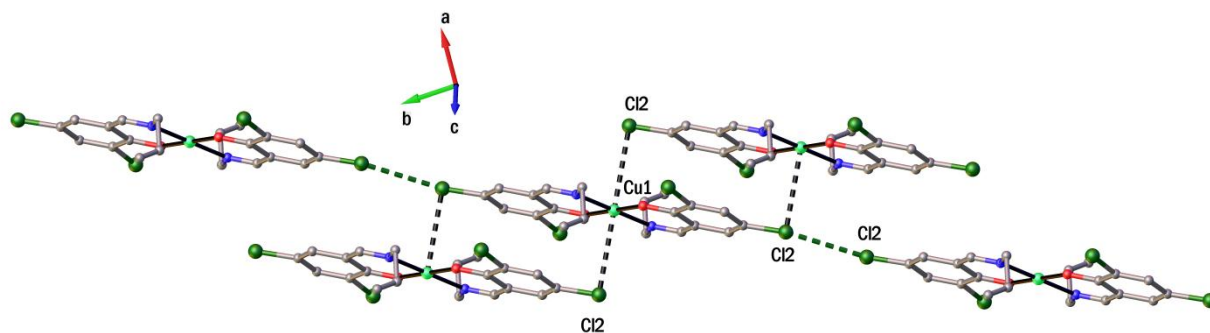
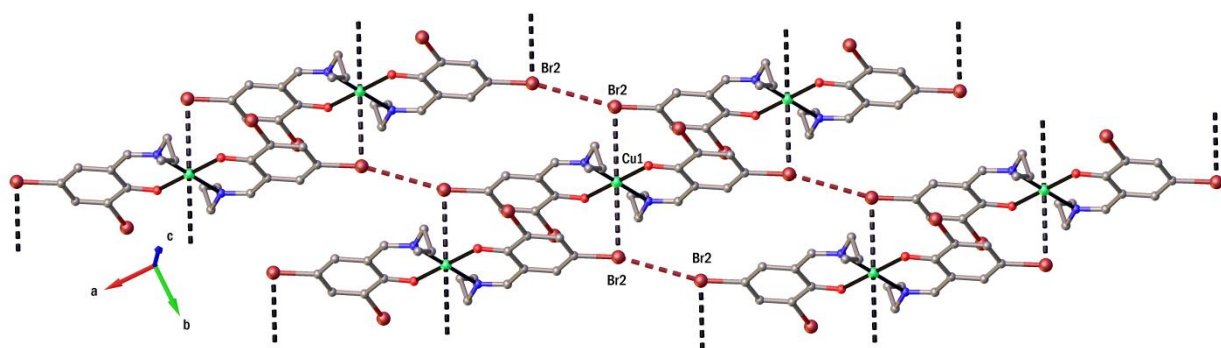


Fig. 5. A side view representation of $(\text{Cl}_2\text{L})_2\text{Cu}$, showing the association of the adjacent molecules through intermolecular halogen...halogen and halogen...Cu interactions.

a)



b)

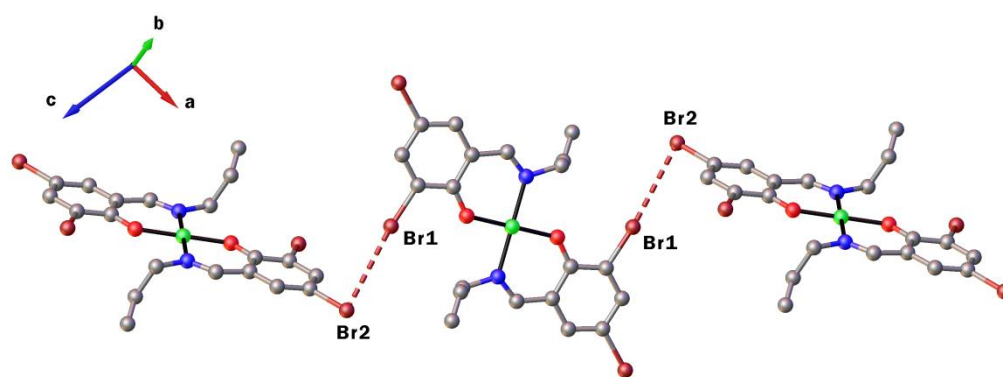


Fig. 6. A side view representation of $(\text{Br}_2\text{L})_2\text{Cu}$, showing the association of the adjacent molecules through: a) intermolecular *para*-halogen... *para*-halogen and halogen...Cu interactions and b) *ortho*-halogen...*para*- halogen interaction.

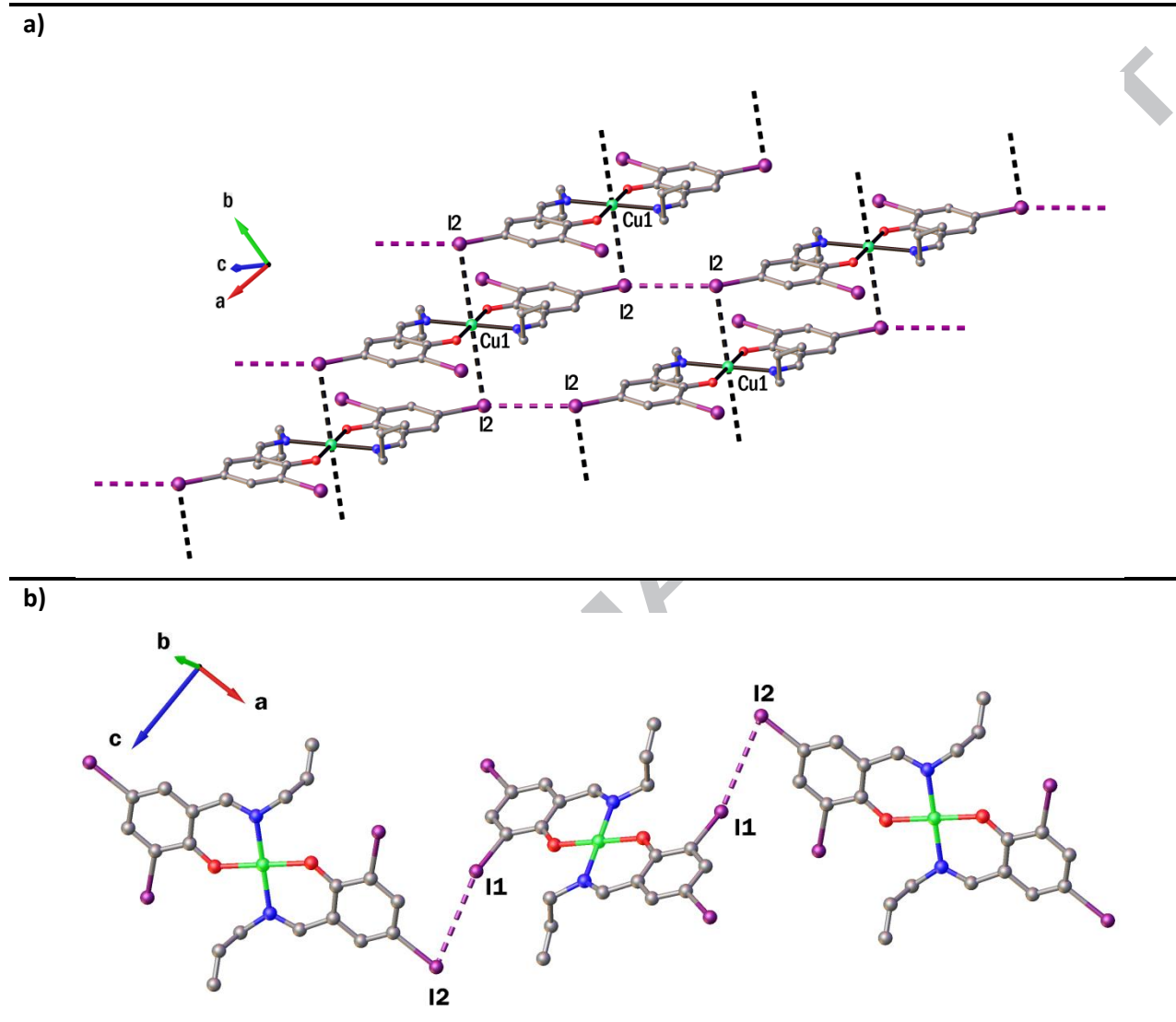
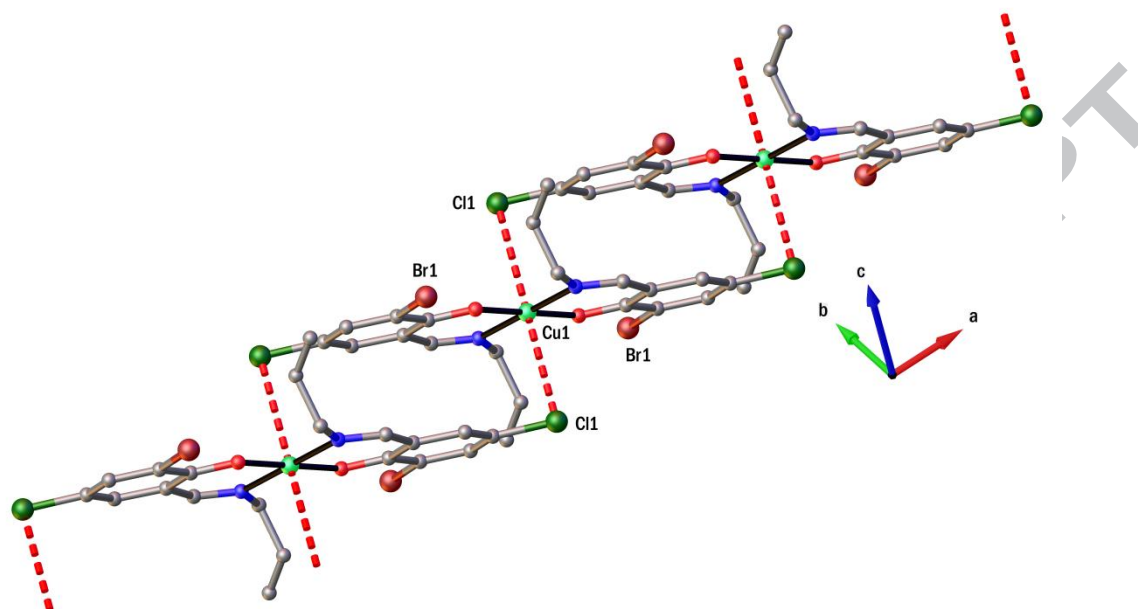


Fig. 7. A side view representation of $(I_2L)_2Cu$, showing the association of the adjacent molecules through: a) intermolecular *para*-halogen...*para*-halogen and halogen...Cu interactions and b) *ortho*-halogen...*para*-halogen interaction.

a)



b)

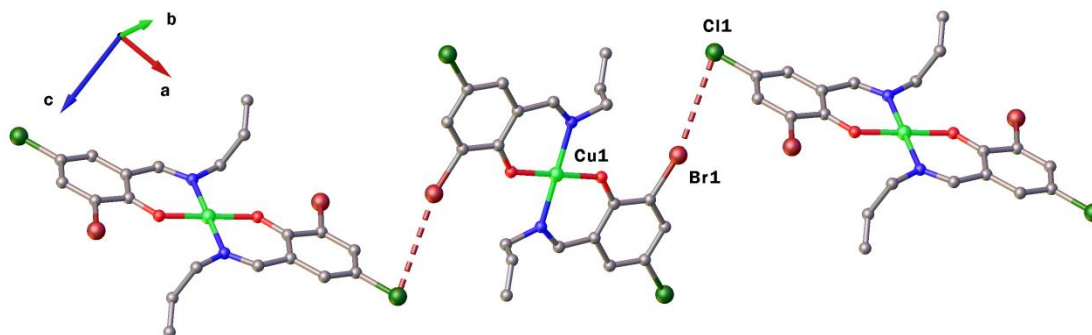


Fig. 8. A side view representation of $(\text{BrClIL})_2\text{Cu}$, showing the association of the adjacent molecules through: a) halogen...Cu interaction and b) *ortho*-halogen...*para*-halogen interaction.

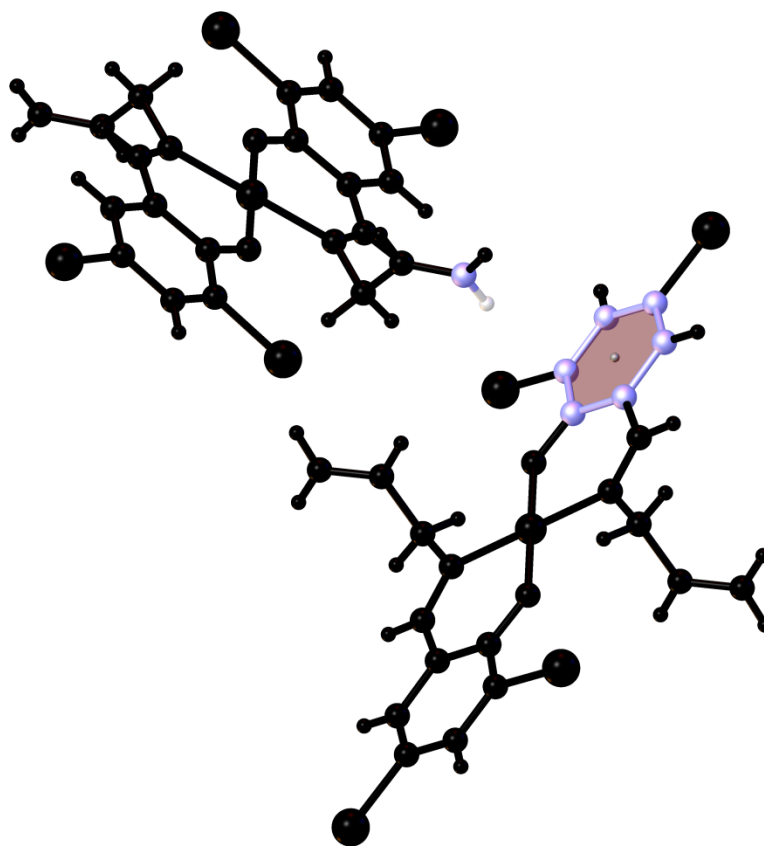


Fig. 9. General illustration of C—H... π interactions in molecular structure of synthesized Cu(II) complexes

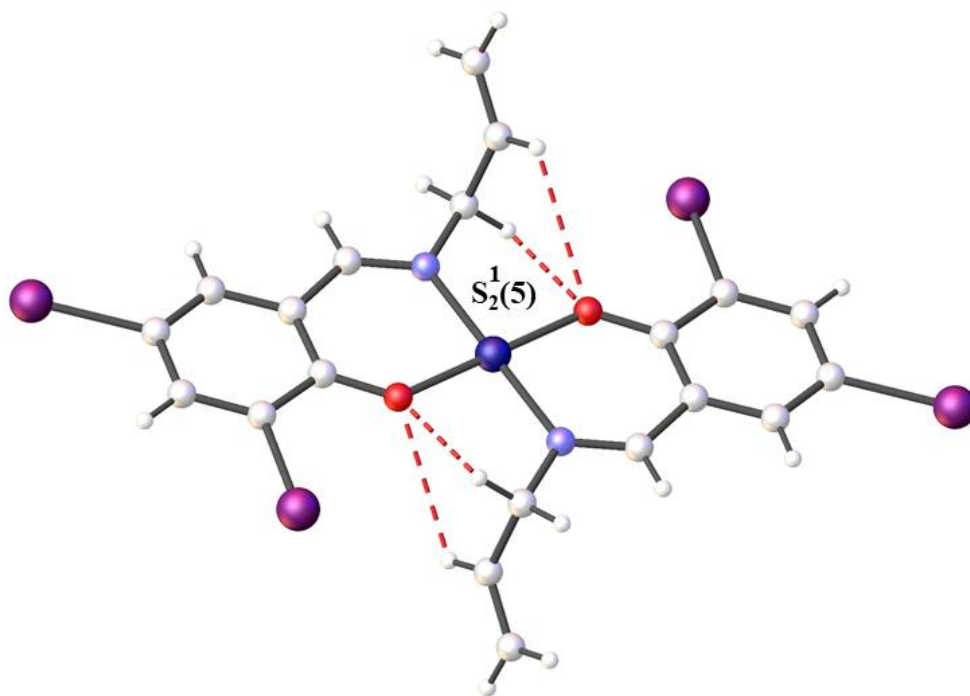


Fig. 10. A general representation of weak intramolecular =CH...O and -CH...O interactions in Cu(II) complexes.

ACCEPTED MANUSCRIPT

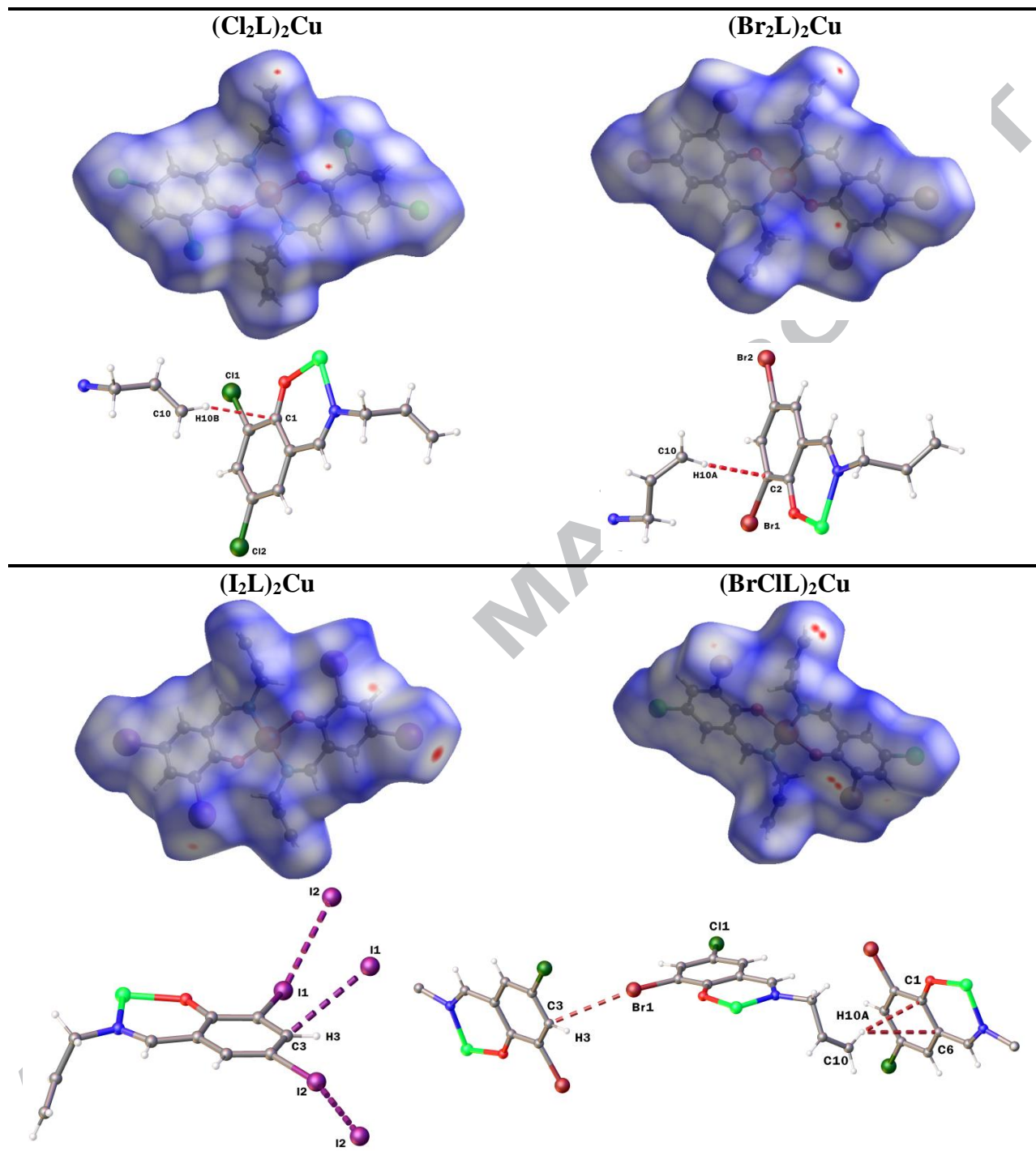


Fig. 11 Hirshfeld surface of **complexes** mapped with d_{norm} . ESP (Electrostatic potential) plotted on Hirshfeld surface mapped from -0.0159 au (red) to 1.2054 au (blue).

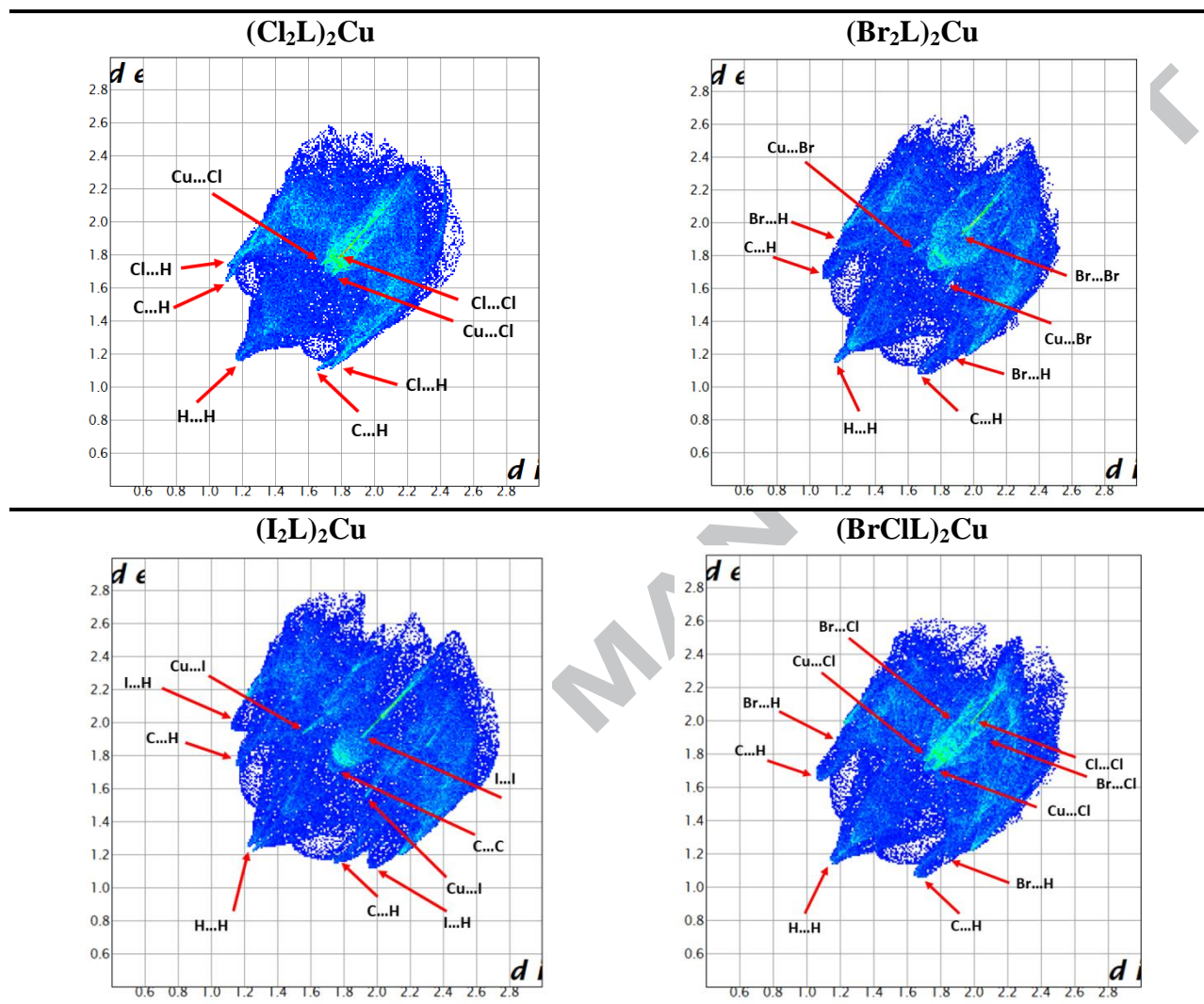


Fig. 12 Hirshfeld surface associated fingerprint plots of complexes: red arrows indicate the spikes of the respective contacts in the crystal packing.

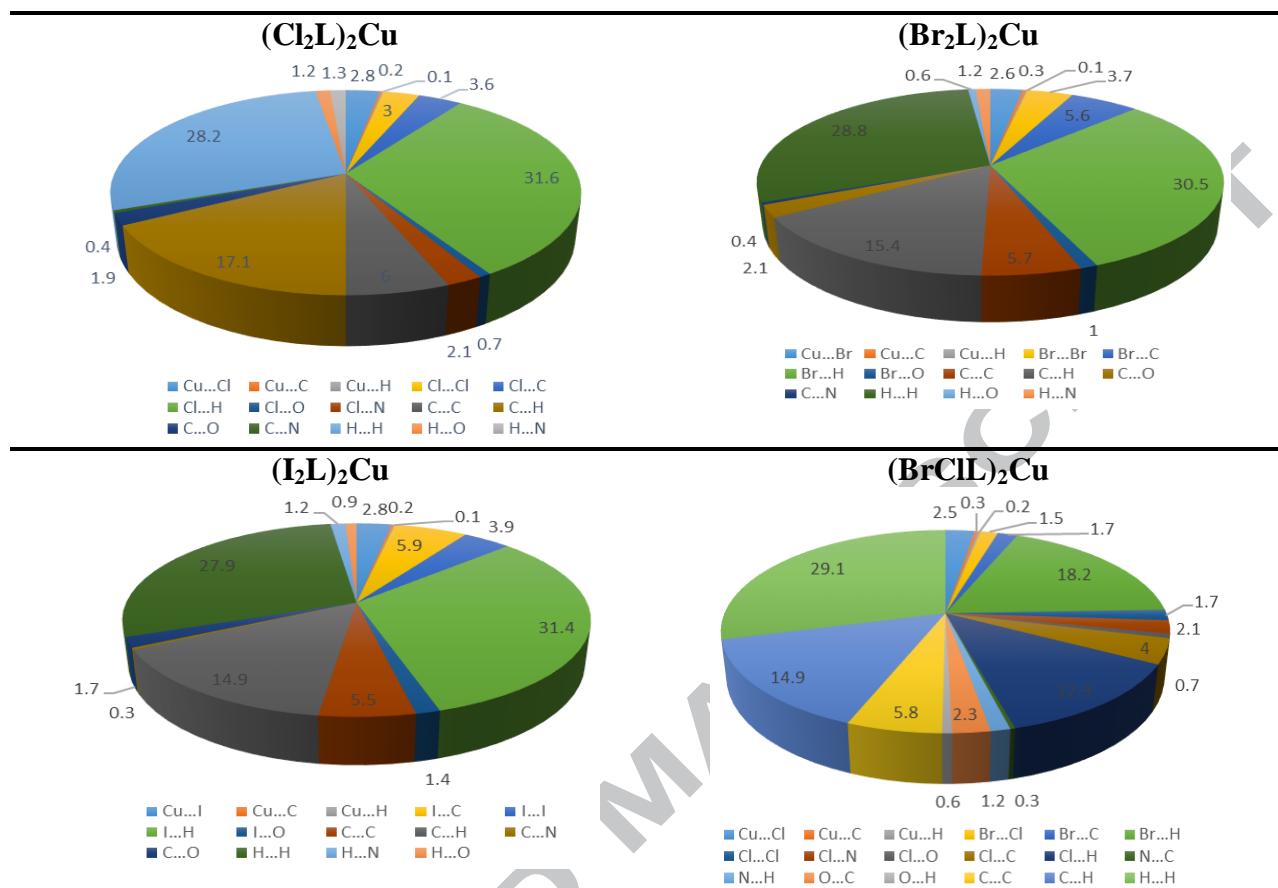


Fig. 13 Relative contributions of different atom-atom contact in the crystal packing of Cu(II) complexes.

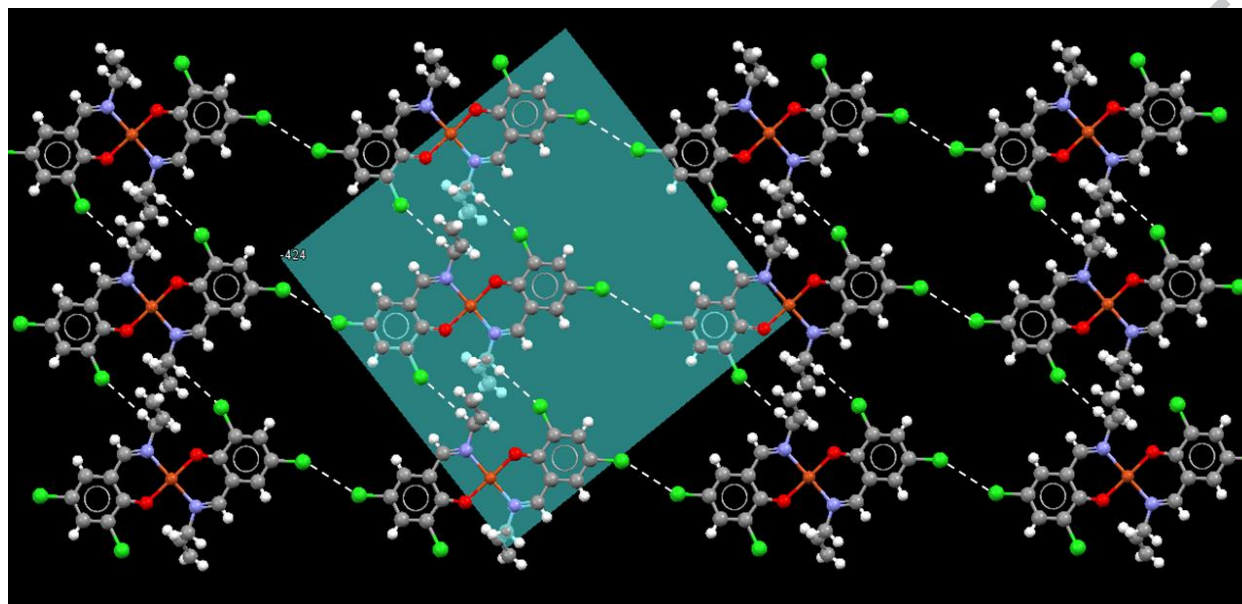


Fig. 14 Supramolecular 2D assembly in (-424) plane determined by Cl..Cl and Cl..H interactions

ACCEPTED MANUSCRIPT

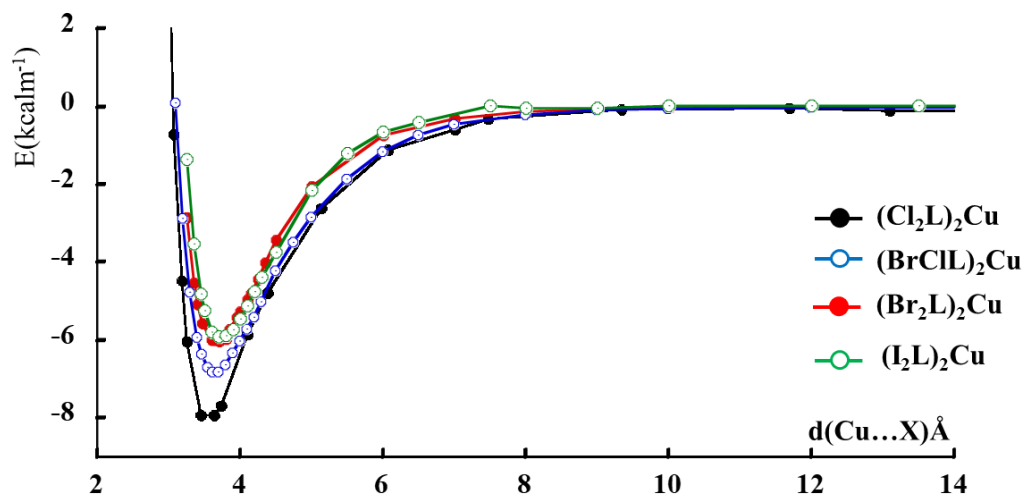


Fig. 15 Energy diagram of Metal-halogen plus π - π interactions with structural parameter at minimum.

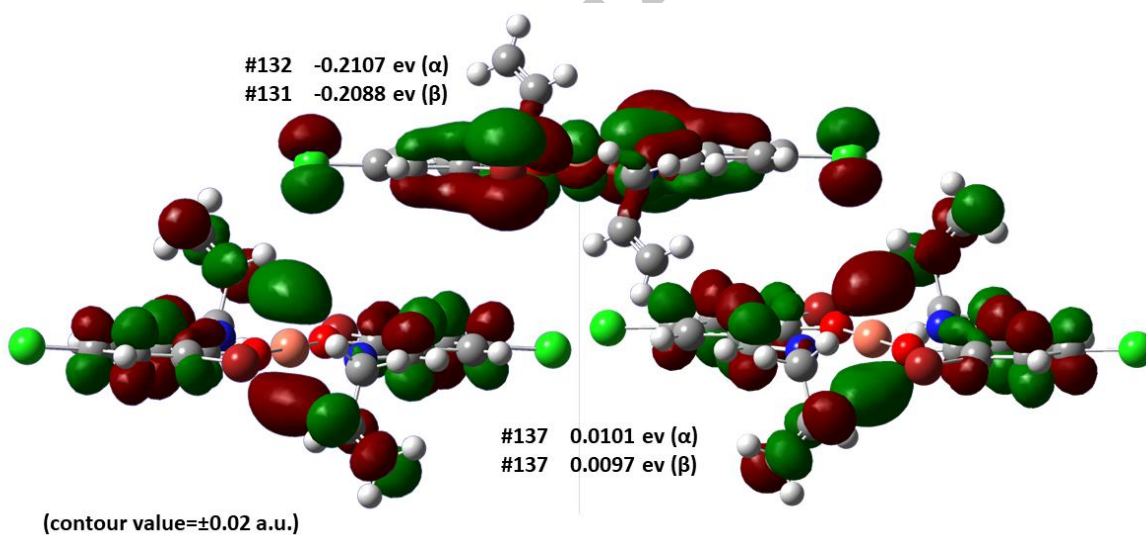


Fig. 16 MO from monomeric species illustrating the copper-halogen interactions.

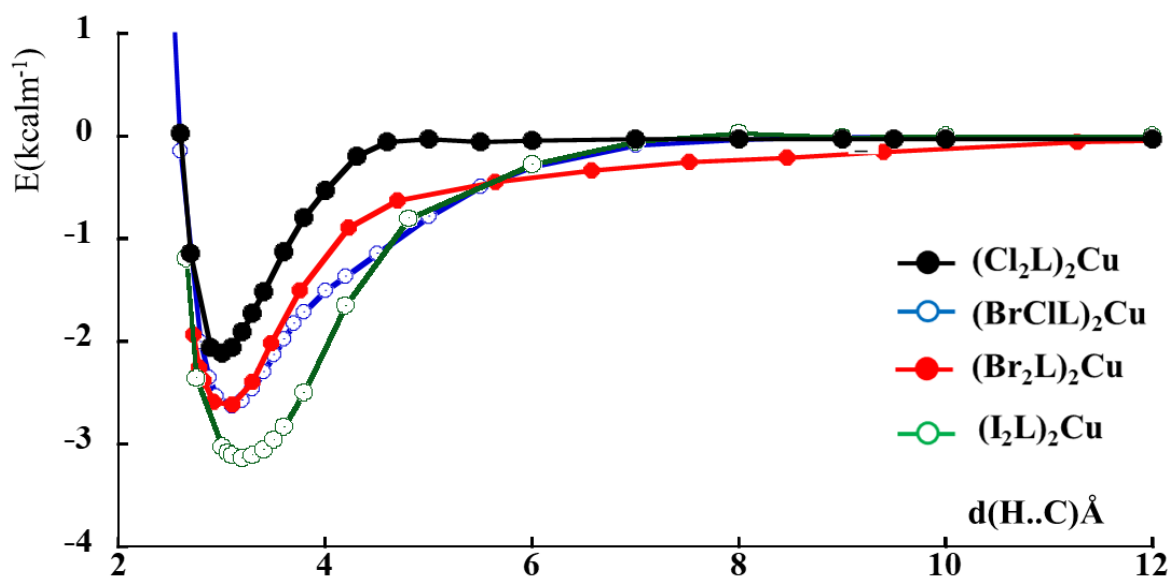


Fig. 17 Energy diagram for $\text{CH}_2\cdots\pi$ interaction

ACCEPTED MANUSCRIPT

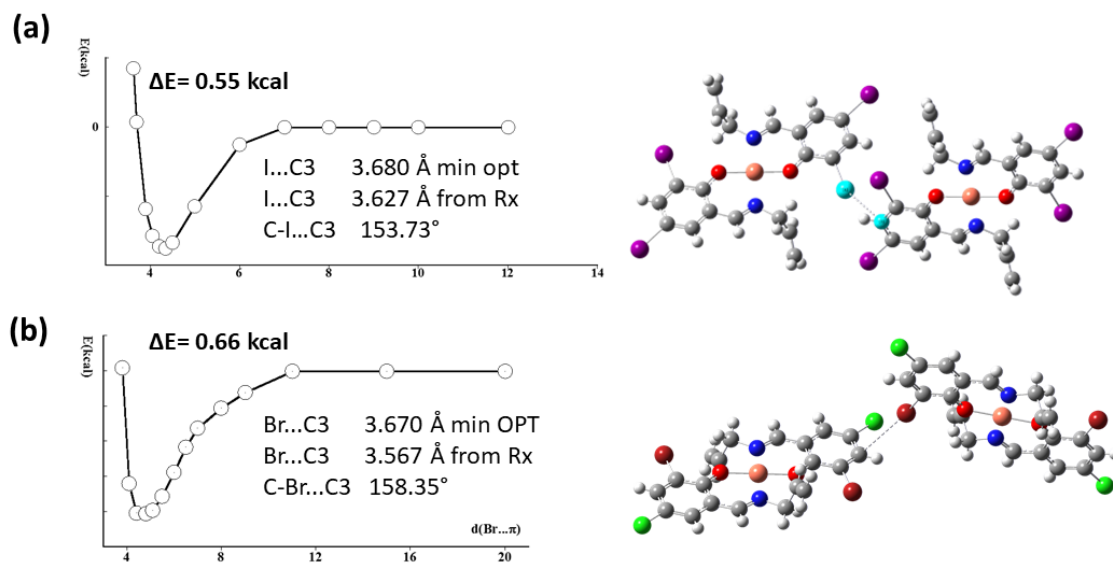


Fig. 18 Energy diagram for halogen.. π interactions in a) $(I_2L)_2Cu$ and b) $(BrCIL)_2Cu$

Table 1. Crystal data and structure refinement.

	(Cl₂L)₂Cu	(Br₂L)₂Cu	(I₂L)₂Cu	(BrClIL)₂Cu
Empirical formula	C ₂₀ H ₁₆ Cl ₄ CuN ₂ O ₂	C ₂₀ H ₁₆ Br ₄ CuN ₂ O ₂	C ₂₀ H ₁₆ CuI ₄ N ₂ O ₂	C ₂₀ H ₁₆ Br ₂ Cl ₂ CuN ₂ O ₂
Formula weight	521.69	699.53	887.49	610.61
Temperature (K)	298(2) K	298(2) K	298(2) K	298(2) K
Wavelength (Å)	0.71073 Å	0.71073 Å	0.71073 Å	0.71073 Å
Crystal system	Triclinic	Monoclinic	Monoclinic	Monoclinic
Space group	<i>P</i> -1	<i>P</i> 2 ₁ / <i>c</i>	<i>P</i> 2 ₁ / <i>c</i>	<i>P</i> 2 ₁ / <i>c</i>
Unit cell dimensions				
a(Å)	8.0165(16)	8.1250(16)	8.3735(17)	8.0578(16)
b(Å)	8.1493(16)	8.4101(17)	8.4803(17)	8.4047(17)
c(Å)	8.6251(17)	15.981(3)	16.502(3)	15.870(3)
α (°)	93.57(3)			
β (°)	111.65(3)	95.90(3)	93.75(3)	95.83(3)
γ (°)	94.98(3)			
Volume (Å ³)	519.0(2)	1086.3(4)	1169.3(4)	1069.2(4)
Z	1	2	2	2
Density (calculated) (Mg/m ³)	1.669	2.139	2.521	1.897
Absorption coefficient (mm ⁻¹)	1.587	8.382	6.233	5.028
F(000)	263	670	814	598
Theta range for data collection (°)	2.96 to 28.37	2.56 to 26.24	2.70 to 24.99	2.58 to 29.17
Index ranges	-10 ≤ h ≤ 10 -10 ≤ k ≤ 10 -11 ≤ l ≤ 11	-11 ≤ h ≤ 11 -11 ≤ k ≤ 11 -21 ≤ l ≤ 21	-9 ≤ h ≤ 9 -10 ≤ k ≤ 9 -19 ≤ l ≤ 19	-11 ≤ h ≤ 11 -11 ≤ k ≤ 11 -19 ≤ l ≤ 21
Reflections collected	21209	10081	7183	9918
Independent reflections	2593 [R _(int) = 0.0349]	2924 [R _(int) = 0.0691]	2048 [R _(int) = 0.1334]	2877 [R _(int) = 0.0366]
Data Completeness (%)	99.8 %	99.9 %	99.9 %	99.9 %
Refinement method	Full-matrix least-squares on <i>F</i> ²	Full-matrix least-squares on <i>F</i> ²	Full-matrix least-squares on <i>F</i> ²	Full-matrix least-squares on <i>F</i> ²
Data / restraints / parameters	2593 / 0 / 133	2924 / 0 / 133	2048 / 0 / 133	2877 / 0 / 133
Goodness-of-fit on <i>F</i> ²	1.037	1.019	1.007	1.046
Final R indices [I > 2σ (I)]	R ₁ = 0.0458 wR ₂ = 0.1081	R ₁ = 0.0382 wR ₂ = 0.0905	R ₁ = 0.0757 wR ₂ = 0.1837	R ₁ = 0.0347 wR ₂ = 0.0825
R indices (all data)	R ₁ = 0.0580 wR ₂ = 0.1202	R ₁ = 0.0527 wR ₂ = 0.0964	R ₁ = 0.0825 wR ₂ = 0.1884	R ₁ = 0.0446 wR ₂ = 0.0863
Largest diff. peak and hole (e.Å ⁻³)	0.492 and -0.671	0.825 and -0.630	2.409 and -2.716	0.411 and -0.965

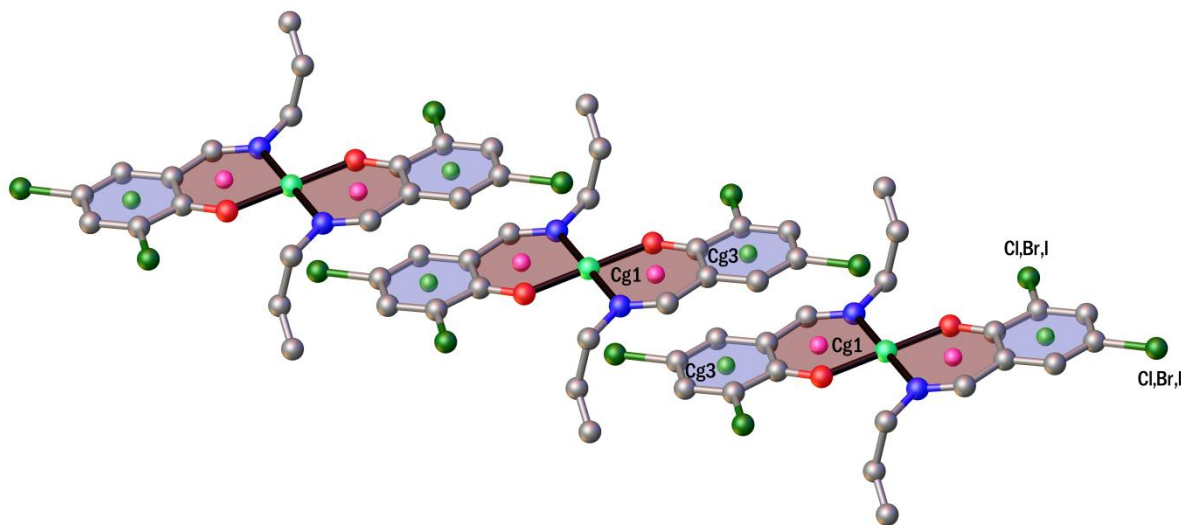
Table 2. Selected bond distances (Å) and angles (°)

	(Cl ₂ L) ₂ Cu	(Br ₂ L) ₂ Cu	(I ₂ L) ₂ Cu	(BrCIL) ₂ Cu
Cu(1)—O(1)	1.895(2)	1.901(2)	1.919(7)	1.9055(17)
Cu(1)—N(1)	2.002(3)	2.002(3)	2.019(8)	2.007(2)
C(7)—N(1)	1.280(4)	1.288(4)	1.294(13)	1.283(3)
C(9)—C(10)	1.276(6)	1.306(6)	1.300(2)	1.300(4)
O(1)-Cu(1)-N(1) [#]	88.60(10)	88.83(10)	89.4(3)	88.87(7)
O(1)-Cu(1)-N(1)	91.40(10)	91.17(10)	90.6(3)	91.13(7)
C(8)-N(1)-Cu(1)	120.50(19)	120.3(2)	120.4(6)	120.21(15)
C(1)-O(1)-Cu(1)	130.4(2)	130.9(2)	130.5(6)	130.57(14)
C(7)-N(1)-Cu(1)	124.5(2)	125.0(2)	124.6(6)	124.94(15)
N(1)-C(7)-C(6)	127.6(3)	126.9(3)	128.2(9)	127.2(2)

[#] Symmetry transformations used to generate equivalent atoms: -x,-y+1,-z for (Cl₂L)₂Cu; -x,-y,-z for (Br₂L)₂Cu, (I₂L)₂Cu and (BrCIL)₂Cu

Table 3. Halogen...Halogen short contact

Crystal	C—X...Y—C	X...Y/Å	C—X...X/°	symmetry	type
(Cl ₂ L) ₂ Cu	C4-Cl2...Cl2 -C4	3.5639	152.63	1-x,3-y,-z	I
(Br ₂ L) ₂ Cu	C2-Br1...Br2-C4	3.8922	156.43	1-x,1/2+y,-1/2-z	I
	C4-Br2...Br2 -C4	3.8610	157.95	2-x,1-y,-z	I
(I ₂ L) ₂ Cu	C2-I1...I2-C4	4.0633	157.71	1-x,1/2+y,-1/2-z	I
	C4-I2...I2 -C4	3.8260	158.32	2-x,-y,-z	I

Table 4 Aromatic interaction parameters (Å and °) for description of π - π interaction in Cu(II) complexes

Cg(I)–Cg(J)	$d_{\text{Cg-Cg}}$ ^a	α ^b	β, γ ^c	$d_{\text{plane-plane}}$ ^d	d_{offset} ^e	Symmetry codes
(Cl₂L)₂Cu						
Cg(1)...Cg(2)	3.6502	2.620	22.17, 23.96	3.3357, 3.3804	1.377, 1.483	-X,2-Y,-Z
Cg(2)...Cg(2)	3.5273	0	17.10, 17.10	3.3713, 3.3713	1.037	-X,2-Y,-Z
(Br₂L)₂Cu						
Cg(1)...Cg(2)	3.6593	2.886	20.89, 22.87	3.3717, 3.4188	1.304, 1.422	1-X,2-Y,-Z
Cg(2)...Cg(2)	3.5870	0	17.82, 17.82	3.4150, 3.4150	1.098	1-X,2-Y,-Z
(I₂L)₂Cu						
Cg(1)...Cg(2)	3.7488	3.132	23.47, 24.84	3.4019, 3.4386	1.575, 1.493	1-X,1-Y,-Z
Cg(2)...Cg(2)	3.5638	0	15.07, 15.07	3.4414, 3.4414	0.926	1-X,1-Y,-Z
(BrClIL)₂Cu						
Cg(1)...Cg(2)	3.6465	3.093	20.58, 23.21	3.3514, 3.4137	1.437, 1.282	1-X,2-Y,-Z
Cg(2)...Cg(2)	3.5918	0	18.64, 18.64	3.4034, 3.4034	1.148	1-X,2-Y,-Z

^a Centroid–centroid distance. ^b Dihedral angle between the ring plane. ^c Offset angles: angle between Cg(I)–Cg(J) vector and normal to plane I, angle between Cg(I)–Cg(J) vector and normal to plane J ($\beta = \gamma$ when $\alpha = 0$). ^d Perpendicular distance of Cg(I) on ring J and perpendicular distance of Cg(J) on ring I. ^e Horizontal displacement between Cg(I) and Cg(J), two values if the two rings are not exactly parallel ($\alpha \neq 0$). For Cg(1): centroid of Cu(1)–O(1)–C(1)–C(6)–C(7)–N(1); Cg(2): centroid of C(1)–C(2)–C(3)–C(4)–C(5)–C(6).

Graphical abstract

Four halogenated Schiff base compounds were synthesized by reaction of halogenated salicylaldehydes (3,5-dichlorosalicylaldehyde, 3,5-dibromosalicylaldehyde, 3,5-diiodosalicylaldehyde and 3-bromo-5-chlorosalicylaldehyde) with allyl amine in water as green solvent at ambient temperature. Their Cu(II) Schiff base complexes showed halogen-halogen, π - π , CH- π interactions and also metal-halogen secondary bonds in crystal packing. These interactions investigated by Hirshfeld surface analysis and theoretical calculations.

